An Analysis of Flow Characteristics of Unconventional Weaving Traffic: Western Cape Case Study.

By

Mathabo Kgabo Sheron Masegela

Research Project presented in partial fulfilment of the requirements for the degree of Master of Engineering in the Faculty of Engineering at Stellenbosch University.

Supervisor: Mrs Megan Bruwer

March 2021

Declaration

By submitting this research project electronically, I declare that the entirety of the work contained therein is my own, original work, that I am the sole author thereof (save to the extent explicitly otherwise stated), that reproduction and publication thereof by Stellenbosch University will not infringe any third party rights and that I have not previously in its entirety or in part submitted it for obtaining any qualification.

March 2021

Abstract

The objective of this study is to analyse the characteristics of unconventional weaving behaviour of traffic within freeway sections and propose remedial measures. Thereby gaining a more detailed understanding of unconventional weaving behaviour, causes and possible solutions. Unconventional weaving traffic is defined as weaving that is not conventional according to the definition in the USA Highway Capacity Manual. It refers to excessive lane changing or weaving that occurs as a result of the geometry of the road, illegal behaviour, disregard of traffic marking etc. For purposes of this study the South African National Road N1 in the Western Cape between the R300 on-ramp and the Okavango Boulevard was selected as the case study. The section of the road under consideration experiences a high number of unconventional weaving manoeuvres resulting from the short distance between successive on-ramps (R300, Okavango), an observed general disregard of the lane markings by numerous motorists (at the R300 on-ramp diverge point) and geometry of the section of road (particularly because no auxiliary lanes are provided). A regression analysis together with fundamental traffic flow diagrams are developed and applied to the base case and proposed remedial actions. The results indicate that weaving within the case study area can be improved by increasing the capacity of the R300 onramp and maintaining a lane balance. It is also observed that weaving within this section is not only related to the operations of the road but is also linked to human behaviour that may not be modelled.

Opsomming

Die doelstelling van hierdie studie is om onkonvensionele weef gedrag in verkeer te analiseer vir ’n spesifieke problematiese gevallestudie en om regstellende maatreëls voor te stel. Sodoende kan ’n beter begrip verkry word in verband met onkonvensionele weef gedrag. Onkonvensionele weef gedrag word gedefinieer as weef gedrag wat nie as konvensioneel beskou word binne die VSA ‘Highway Capacity Manual’ nie. Dit verwys na oormatige baan verwisseling wat plaasvind as gevolg van pad uitleg, onwettige rygedrag, verontagsaming van verkeersmerke en verkeerstekens, ens. Die Suid-Afrikaanse nasionale weg, N1 in die Weskaap tussen die R300 oprit en die Okavango Boulevard is verkies vir hierdie gevallestudie. Op hierdie deel van die snelweg vind ’n hoe mate van onkonvesionele weef gedrag plaas as gevolg van die kort afstand tussen opeenvolgende opritte (R300, Okavango), ’n opvallende algemene verontagsaming van die baan merke deur baie motoriste (by die R300 oprit divergeer punt) en die geometrie van die stuk pad(veral omdat daar geen addisionele afvoer bane bestaan nie). ’n Regressie analise tesame met fundamentele verkeersvloei diagramme word ontwikkel en word toegepas op die huidige basis situasie asook tot die nuwe voorgestelde verbeterde situasie. Die resultate toon aan dat weef gedrag in die gevallestudie area verbeter kan word deur middel van ’n vergroting van kapasiteit van die R300 oprit en deur middel van ’n behoud van baan balans. Wat ook waargeneem word is dat weef gedrag binne die gevallestudie area nie net aan die pad werking gekoppel kan word nie, maar ook aan menslike rygedrag wat nie gemodelleer is nie.

ACKNOWLEDGEMENT

I would like to thank my supervisor Mrs. Megan Bruwer and my family for their assistance with the research project and without whom I would not have completed the master's degree. I am thankful for the team at SANRAL Western Region for availing data for my research. Finally, I am thankful for my sponsors BVi Consulting Engineers and Roads Agency Limpopo SOC Ltd for funding my degree.

TABLE OF CONTENTS

LIST OF FIGURES

LIST OF TABLES

LIST OF PHOTOS

LIST OF ABBREVIATIONS

HCM	: Highway Capacity Manua;l
TRB	: Transportation Research Board
PTV AG	: Planung Transport Verkehr AG
NCHRP	: National Cooperative Highway Research Program
MLC	: Mandatory Lane Change
DLC	: Discretionary Lane change
LOS	: Level of Service
FHWA	: Federal Highway Administration
SANRAL	: South African National Roads Agency Soc Limited
SSML	: Stellenbosch Smart Mobility Lab
CCTV	: Closed Circuit Television
VDS	: Vehicle Detection System
GA	: General Algorithm
HOV	: High Occupancy Vehicle
HGV	: Heavy Goods Vehicle

1 INTRODUCTION

1.1 Background to study

In current times, emphasis in transportation is shifting to focus on dynamic aspects such as improvement of traffic flow as opposed to concentrating on the static aspects, such as infrastructure design. (Kusuma, 2015) (Zhang, 2005) . An in-depth understanding of the interaction between traffic flow and the static aspects is becoming realised, for reasons of, amongst others, efficiency and safety.

The focus on traffic flow includes studies into congestion, queue length and bottleneck formations amongst other aspects. The studies also consider how these aspects are affected by road design. Studies have shown that road capacity tends to be reduced at areas where quick human response is required such as at intersections, merging and at weaving sections (Kou & Machemehl, 1997).

Weaving sections are defined by the Highway Capacity Manual (HCM) of the Transportation Research Board (TRB), (HCM, 2010) as sections at which two flows in the same direction cross without the help of a traffic control device. These sections create rapid lane changing manoeuvres, which result in conflict and significantly reduced capacities. As alluded to earlier, weaving is significantly affected by the road's geometric configuration. Such interactions are often observed in areas where merging and diverging sections follow each other in short succession. Merging occurs when traffic flowing from an on-ramp joins the mainstream of the freeway and where an off-ramp is a relatively short distance from the on-ramp.

Weaving and merging sections are important traffic bottlenecks and an understanding of the dynamics involved at these facilities is paramount in guiding road design. The characteristics of weaving behaviour within weaving segments are covered extensively in literature (Zhang, 2005) (Abraghan, 2016). These segments are known for operational and safety problems and require complex designs and complex decision-making during manoeuvres. However, there is limited research into weaving manoeuvres (hereby referred as the crossing of two flows in the same direction) resulting from operational and structural constraints. For purposes of differentiation, weaving manoeuvres and weaving segments that are specifically classified in HCM (2010) will be referred as conventional weaving and those introduced in this paper (resulting from operational conditions and structural constraints) as unconventional weaving.

The constraints or instigators of weaving manoeuvres within unconventional weaving segments can be a result of the road markings, locations of the dedicated lanes and due to

human behaviour. This research aims at characterising the traffic behaviour of weaving vehicles within these constraints.

1.2 Description of the main problem

The number and frequency of potential vehicular conflicts occurring within conventional and unconventional weaving sections make them difficult sections to travel through. Traffic movement in these sections tend to be defined by decreased vehicle speeds, increased congestion and reduced freeway segment capacity. Added to this, studies have shown that there is a higher rate of accidents within weaving segments as opposed to other freeway segments. The occurrence of accidents was found to be related to the type of movement performed by the vehicle within the weaving segment and the segment configuration (Golob, et al., 2004). Although there are no studies linking the rate of accidents within unconventional weaving segments, the hypothesis brought forth in this study is that there is a higher rate of accidents within these segments.

A deeper understanding of the characteristics of traffic within these segments may hold a solution to the increased accident rates. As this research aims to understand and classify the characteristics of traffic, it circuitously addresses safety and efficiency of these segments.

1.3 Objectives of the research

The aim of the research is to, aided by a case study, assess the behaviour of traffic at a problematic section with regard to unconventional weaving behaviour within the Western Cape and propose remedial actions. Thereby gaining a more detailed understanding of unconventional weaving behaviour and possible solutions.

The aim will be achieved by following the research objectives listed henceforth:

- Gaining an understanding of the difference between a conventional and unconventional weaving behaviour.
- Identifying a region within Western Cape Province that exhibits unconventional weaving behaviour.
- Collecting and analysing traffic data using different methods to assess the impacts of the weaving behaviour on the operations and safety on the case study.
- Selecting appropriate modelling and analytical tools to replicate the operations on the case study.
- Proposing and modelling remedial actions that would improve operations and safety issues identified on the case study.
- Making recommendations of proposed solutions to the identified weaving behaviour and safety issues.

1.4 Scope limitation

It is acknowledged that characteristics of weaving traffic within the discussed segments is affected by the downstream and upstream traffic conditions, which will differ from case to case. This research will only look at one case with various constraints that create unconventional weaving manoeuvres. There are countless operational constraints that could lead to weaving which are not covered in this report. There is therefore scope to expand this research to consider further examples on unconventional weaving.

1.5 Plan of development

A brief overview of the literature (in Chapter 2) available on weaving segments and the different traffic flow models that may be used to characterize and assess weaving traffic will be provided. The literature review also includes a discussion of the simulation software that is used in this research study to assess traffic in weaving areas. Chapter 3 discusses the case study that forms the basis of analysis in this research. Chapter 4 describes the m7ethodology that will be used in acquiring, processing, analysis and interpretation of the available data. The development of the analysis model will be discussed in Chapter 5 followed by model calibration and validation in Chapter 6. In Chapter 7 an assessment of possible actions that may mitigate identified operational constraints is given and the effects that these actions will have on the freeway segment will be provided. The discussions and conclusions are presented in Chapters 8 and 9, respectively.

2 LITERATURE REVIEW

2.1 Introduction

According to the Highway Capacity Manual, weaving occurs when traffic from different streams, in the same direction cross paths without being aided by traffic control devices (TRB, 2010. Weaving sections tend to have greater levels of conflicts and high turbulence. The turbulence creates operational difficulties and requirements. These complex operations necessitate complex sets of decisions and actions such as gap search, speed reduction, lane changing and speed adjustment. Weaving sections are known to have low capacity and high time headway (HCM, 2010).

2.2 Types of weaving sections

Weaving sections are classified by the road configuration and the number of lane changes required (Zhang, 2005). The capacity of the weaving area is usually analysed based on the weaving configurations, no of lane changes and the speed of vehicles within these areas. In the HCM (1985) (Also cited in Richard *et al.*, (2001) three weaving configurations are defined depending on the number of lane changes required to complete a weaving manoeuvre. Weaving type A is classified as a ramp weave where each weaving vehicle must make only one lane change. Weaving types B and C are classified by one weaving movement that can be made without requiring a vehicle to make a lane change action. In Type B weaving, the other weaving movement is achieved by changing lanes only once, while Type C weaving will require a lane change over two or more lanes

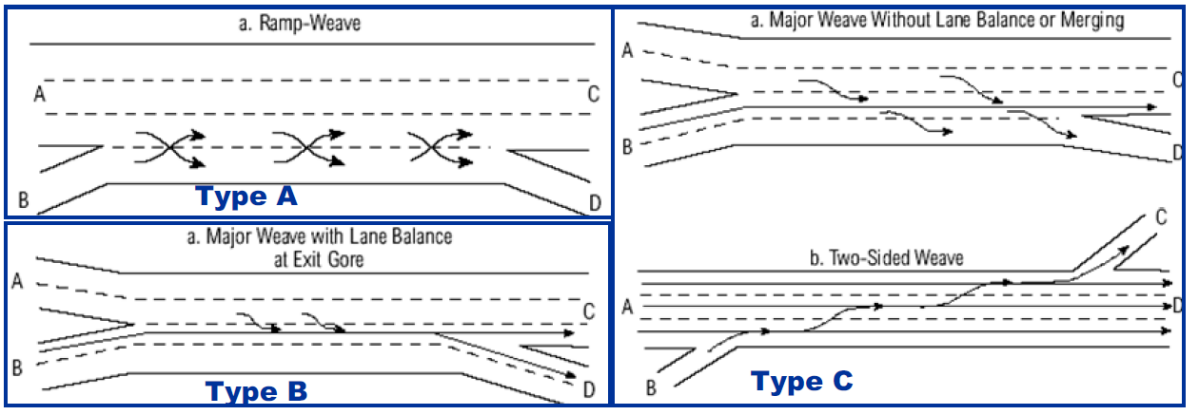

Figure 2-1: Types of weaving (HCM, 2010)

2.3 Safety aspects of weaving sections

A study has been performed to provide a statistical analysis of accidents that happen in weaving sections by comparing them to those of other freeway sections. In his study Golob *et al.* (2003) supports the hypothesis that there are higher rates of accidents within

weaving sections. The research distinguished between the kind of accident likely to occur and the time that accidents are likely to occur for different types of weaving sections.

According to Golob *et al.* (2003), for type A weaving sections, the most likely accident is a rear-end accident that occurs during off-peak hours at night. The accidents are usually located in an interior lane and are less severe than accidents occurring within Type B and Type C weaving segments. This type of accident is also more likely to occur in wet weather and on slippery road surfaces. Golob *et al.* further reports that Type B weaving section accidents are usually not concentrated on the interior lane and are likely to include vehicles that are in the process of changing lanes. Speed differential has been found as the main factor for accidents on this type of weaving section. Golob *et al.* categorises Type C weaving accidents as most likely to happen on weekday peak-hours periods on the left lane (outer lane). Similar to Type A weaving segments, the accidents occurring in Type C weaving segments are most likely to be rear-end accidents.

2.4 Traffic flow models

Traffic flow is controlled by various aspects such as drivers' behaviour, traffic conditions (i.e. travel speeds, congestion) external situations (such as weather) and the condition of the road infrastructure. Driver behaviours include, inter alia, the desired minimum and maintained headway, the driving speed, drivers experience and age.

Various theories are proposed in literature (Wang *et al.*, 2014; Sarvi *et al.*, 2011) to relate driving behaviour to traffic condition. Most theories distinguish two types of driving tasks: either a longitudinal driving task or a lateral driving task. A longitudinal task refers to acceleration, maintaining distance headway and speed. A lateral task includes overtaking and changing lanes. These two tasks are the basis of most traffic flow models.

Traffic models endeavour to represent and simulate the movement of traffic within a specified section. They may be used to assess the effect that policies, infrastructure and traffic control devices have on traffic. They help determine at what point traffic jams may occur, how the jam propagates, for how long they last and the effect they may have on the downstream traffic. The models are therefore essential in describing the physical propagations of traffic streams and can also be used to improve road safety (Meng, 2006).

The existing traffic flow models follow different schools of thought and approaches, based on whether the models operate in discrete or continuous time, depending on the level of detail and whether the models are stochastic or deterministic. Following (Treiber & Kesting A, 2013) , one can distinguish the propagation models as macroscopic,

mesoscopic, microscopic or sub microscopic. Macroscopic models are based on continuum mechanics that typically follow fluid dynamics models, they have the lowest level of detail and the highest level of aggregation (Van Wageningen-Kassels et al., 2015). This model is used more for analysis of a network in which performance characteristics such as quality and level of service are analysed. Mesoscopic models also have a low level of detail, high level of aggregation and are based on gas kinetic analogy (Hidas, 2005). Microscopic models have a high level of detail and low level of aggregation and describe in detail the interaction between vehicles in a traffic stream (Van Wageningen- Kassels et al., 2015). This research will look at both the macroscopic and microscopic approach with more focus given to the microscopic model.

2.4.1 Macroscopic Models

Macroscopic models are based on continuum mechanics and tend to characterize traffic flow as behaving like gases and liquid that satisfy continuity equations. Traffic in a macroscopic model is described by density, flow and mean speed (Wei & Wanjing., 2013). The low level of detail and low precision makes this model relatively faster to operate than other types. The shortcoming of this model is that it does not compute the behaviour of single vehicles which can impact on the traffic flow and the overall network performance.

2.4.2 Microscopic

Microscopic models operate at a level of a single vehicles. They provide detailed characteristics of each single vehicle such as the position, the speed, velocity, and acceleration. The behaviour of each vehicle is affected by the behaviour of vehicles in the neighbouring traffic stream. These interactions can be defined by different logics, that are discussed in the next section (Wei & Wanjing, 2013). The high-level nature of the microscopic model requires detailed and accurate inputs for estimating the traffic and vehicle trajectory. Vehicle trajectories are not defined; vehicles can automatically choose their preferred trajectory given that the origin and destination are well defined. Weaving manoeuvres are modelled using microscopic models as they require a vehicle-by-vehicle investigation of the trajectory of each vehicle in the traffic stream. Microscopically, the weaving manoeuvre follows three logics: car-following, lane changing and gap acceptance (Wei & Wanjing, 2013). These logics are discussed in the sections below.

2.4.3 Car-following logics

2.4.3.1 *Introduction (Constant headway logics)*

Car-following models describe the reaction a subject driver (also referred to as the following driver) who is following a leading vehicle in reaction to the leading driver's behaviour (Kusuma, 2015). The models focus on the dynamics of a line of vehicles accelerating or decelerating in response to the leading vehicle. Car-following usually occurs on a multi-lane road when overtaking is difficult or unsafe or when traffic is restricted to one lane. There are various car following models which are in consonance with each other and are derived from fundamental formulae. However, in this literature review, focus will be limited to the Wiedemann (PTV AG, 2011) and General Motors models (Higgs, 2011) and a brief description of the Pipes and Forbes models (Gao, 2008).

In 1958, Pipes developed a car-following model that assumed that vehicles following each other maintain a constant distance headway (Soria, 2010). The model suggests that distance between the subject vehicle and the lead vehicles is dependent on the relative speed of the vehicles (Gao, 2008).

Forbes, whose model assumes that cars following each other maintain a constant time headway, followed Pipes' research (Soria, 2010). The model essentially accounts for the time of reaction required for the subject vehicle to perceive and accelerate or decelerate in response to the lead vehicle. The model implies that the reaction time of subject vehicle should be smaller or equal to the time headway between the lead and subject vehicle (Subramanian, 1994; Soria, 2010).

Though both models developed by Pipes and Forbes introduced the concept of car-following, they contained limitations. One large limitation was that both models were found to be inaccurate at low speeds and did not represent field results at these speeds. The two models and other models that are based on constant headway assume that a driver's reaction is exclusively in response to the lead vehicle and excludes the effect of the obstruction or vehicle ahead of the lead vehicle. Various models (Kusuma, 2015; Soria, 2010), have been developed that addresses the limitations of the original models. These models are referred to as stimuli response models (Kusuma, 2015).

Stimuli response models are car-following models based on the premise that the response of a subject vehicle is a function of the sensitivity, stimulus and the reaction time (Soria, 2010). The response is to either accelerate or decelerate in proportion to the stimuli. The reaction time is the time taken to perceive and respond to a situation. Stimuli response generally follows the form of Formula (1). These models have been found to be better estimators of car-following behaviour. General Motors and Weidemann models are types of stimuli response models. The literature review will focus on the General Motors and

Wiedemann car-following models due to extensive studies taken to calibrate these models and because the models are used in microscopic simulation models (such as PTV VISSIM).

$$a(t+\Delta t) = k * [V_n(t) - V_{n+1}(t)] \quad (1)$$

Response *sensitivity* *Stimulus*

Where, α is acceleration, t is time, Δt is the reaction time, $V_n(t)$ and V_{n+1} are the velocity of the subject vehicle (n) and the leading vehicle respectively(n+1).

2.4.3.2 *General Motors model (stimuli response method)*

The schematic diagram, Figure 2-2 and corresponding definitions depict variables that will be used henceforth. In reference to Figure 2-2 consider two vehicles travelling from left to right at the same time. Vehicle n represents the Subject vehicle and vehicle n+1 denotes the lead vehicle. Vehicles n and n+1 are accelerating or decelerating at rates αn and αn+1, respectively. The relative acceleration of the vehicles is denoted as $\Delta\alpha$ which equals α_{n+1} - αn. Since the vehicles change positions, speeds, and acceleration rates over time, the subscript "t" is used to specify time. Δt represents the interval between the stimulus and the reactions time it takes to respond. Therefore t+Δt denotes the time at which an action (acceleration or deceleration) is applied.

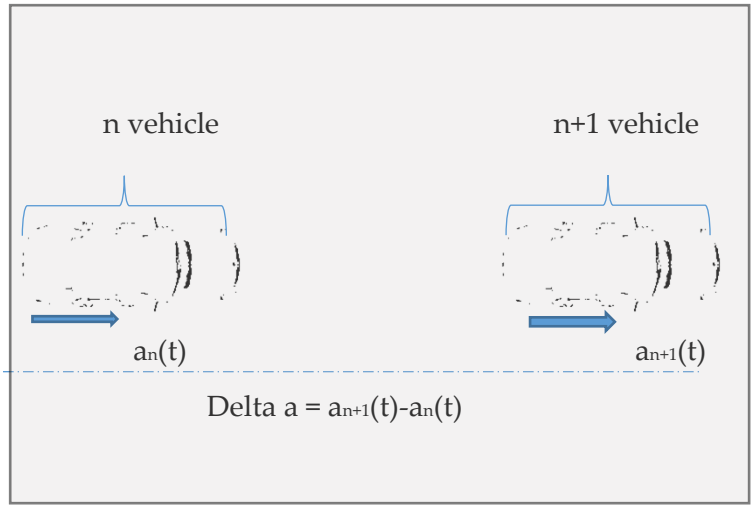

Figure 2-2: Car-Following Model (adopted from (Kusuma, 2015)

Various research efforts have been taken to develop the General Motors model (Higgs, 2011; Soria, 2010). The first research on stimuli response method was undertaken by Chandler *et al.* (1958) who developed a simple model that stated that the desire for a subject vehicle to accelerate or decelerate is depended on the speed differential between the lead and subject

vehicle (Soria, 2010). The model also assumed that sensitivity is constant for both acceleration and deceleration and is inversely proportional to the vehicle mass.

Herman and Rothery (1963) challenged the premise of constant sensitivity and hypothesised that sensitivity is different for accelerating and decelerating vehicles. Gazis *et al.* (1959) found through research that sensitivity is related to the distance between the subject and the lead vehicle. The resultant formula is given in Equation (2). The model implies that sensitivity increases with decreasing relative distance or at smaller headways.

$$a_{n+1}\,(t+\delta t) = \frac{a_{1,m}}{[x_n(t)-x_{(n+1)}(t)]^l}\,[V_n(t)-V_{n+1}(t)] \qquad (2)$$

Where, x_n is subject vehicle's position and x_{n+1} the leading vehicle's position. $\alpha_{1,m}$ is the sensitivity parameter with constants I and m that are calibration parameters.

This model was found to perform poorly in non-congested traffic. Edie (1961) developed a nonlinear model for non-congested traffic. This model related sensitivity to the speed and to the square of the relative distance. The resultant formula is given below:

$$a_{n+1}\,(t+\delta t) = \frac{a_{1,m}V_n}{[x_n(t)-x_{(n+1)}(t)]^{2^l}}\,[V_n(t)-V_{n+1}(t)] \qquad (3)$$

Gazis *et al.* (1961) followed by developing a nonlinear formula that holds true for both congested and non-congested traffic. The proposed General Motors car-following model assumes the following relationship:

$$a_{n+1}\,(t+\delta t) = \frac{a_{1,m}[V_{n+1}(t+\delta t)]^m}{[x_n(t)-x_{(n+1)}(t)]^l}\,[V_n(t)-V_{n+1}(t)] \qquad (4)$$

Response sensitivity stimulus

Where m and l are the speed exponent and distance headway.

2.4.3.3 *Wiedemann (psychophysical logics)*

The Wiedemann method is a psychophysical method that defines the driver's perception threshold in response to the leading vehicle and the regimen formed by these thresholds (also described in Gao, 2008). The premise of the method is that a driver will accelerate until reaching their own perception threshold as a response to slow moving vehicles. Given that they do not know how fast the lead vehicle is driving, the driver will slow down and drive at a speed lower than the lead vehicle until he reached another perception threshold. (PTV AG, 2011) (Mu, 2013).The perception thresholds and regimen are shown in Figure 2-3 and described in the following section.

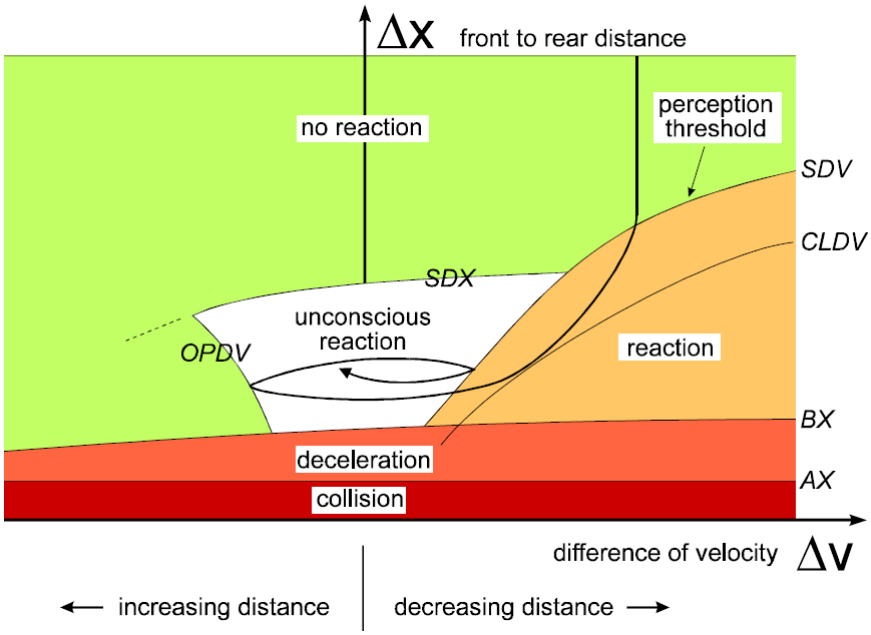

Figure 2-3: Wiedemann Acceleration/Deceleration Threshold (Source: Ptv AG, 2011)

In reference to Figure 2.3 (PTV AG, 2011), AX represents the minimum following distance headway in a congested condition, which is the bumper-to-bumper distance within which collisions occur. BX represents the minimum desired following distance within which the subject vehicle will decelerate to prevent a collision (PTV AG, 2011). The free driving state in which a driver is not inclined to accelerate or decelerate is represented by SDX (PTV AG, 2011). SDV represents the instant at which the driver recognising that the lead vehicle is driving at a slow speed, then in response, the subject vehicle will decelerate to match the speed of the lead vehicle(PTV AG, 2011). The limit for the speed deferential between the subject and lead vehicle is represented by OPDV (PTV AG, 2011).

Wiedemann formulae are derived for the steady state regime where there is no speed differential ($\Delta v=0$) and the vehicle spacing is that desired by the driver ($S_n \approx S_{desired,}$ where

ABX ≤ S_n ≤ SDX). The expected value of the SDX, represented as E(SDX), is formulated below together with other associated formulae.

$$E(AX) = s_j + AX_{add} + AX_{mult} * E(RND1_n) \quad (5)$$

$$E(ABX) = E(AX) + E(BX) * (V)^{0.5} \quad (6)$$

$$E(SDX) = s_j + E(BX) * E(EX)(V)^{0.5} \quad (7)$$

$$BX = BX_{add} + BX_{mult} * RND1_n \quad (8)$$

$$EX = EX_{add} + BX_{mult} * (NRND - RND2_n) \quad (9)$$

$$SDV = \left(\frac{\Delta x - L_n - AX}{CX}\right)^2 \quad (10)$$

$$CX = CX_{const} * [CX_{add} + CX_{mult} * (RND1_n + RND2_n)] \quad (11)$$

Where BX_{add}, BX_{mult}, EX_{add}, EX_{mult}, AX_{add}, AX_{mult}, CX, are calibration parameters. Parameters NRND, RND_2, $RND1_n$ are normally distributed random numbers and driver dependent parameters.

AX which is the minimum following distance headway in a congested condition (standstill traffic) is calculated using Equation 5, which is used to calculate other thresholds. Equation 6, calculates the limit for a desired minimum following distance (Higgs, 2011).

Equation 7 calculated the maximum following distance. Equation 10 is used to calculate the perception threshold (SDV), which is the moment the subject vehicles begins to react to the leading vehicle. Equation 12 represents the reaction threshold curve (OPDV) which is the point of re-acceleration by the subject vehicle while still closing on the leading vehicle (Higgs, 2011).

$$CLDV = \left(\frac{\Delta x - L_n - AX}{CLDVCX}\right)^2 \quad (12)$$

The (OPDV) curve bounds the instinctive reaction regime and represents the point where the subject vehicle realised that there is an increase in distance over time between them and the leading vehicle. As a response, the subject vehicle will desire to maintain a reasonable space headway by acceleration towards the lead vehicle until such headway is achieved. Equation 13 is used to calculate the threshold curve (Higgs, 2011; PTV AG, 2011).

$$OPDV = CLDV * (-OPDV_{add} - OPDV_{mult} * NRND) \quad (13)$$

''Where $OPDV_{add}$ and $OPDV_{mult}$ are calibration parameters. NRND is a normally distributed random parameter'' (PTV AG, 2011).

The discussed thresholds create six regimes. The regimes are free driving regime, approaching regime, closely approaching regime, the deceleration following regime, the acceleration following regime and the emergency regime (Higgs, 2011). Within the free driving regime, the subject vehicle is driving and accelerating at the desired speed without interference from the lead vehicle. The subject vehicle acceleration is calculated using Equation—14 . (Higgs, 2011; PTV AG, 2011).

$$b_{max} = BMAX_{multi} * (V_{max} - v * FaktorV) \quad (14)$$

$$FAKTORV = \frac{V_{max}}{V_{des} + FAKTORVmult * (V_{max} - V_{des})} \quad (15)$$

Where $FAKTORV_{mult}$, $BMAX_{mult}$ are calibration parameters.

The approaching regime occurs when the subject vehicle in the free driving regime reaches and passes the perception threshold (PTV AG, 2011). In this case the vehicle will slow down as per Equation 16. The next regime is the closely approaching regime which happens when a subject vehicle reaches and passes the next threshold i.e. the closing difference in velocity threshold (CDV). When the vehicle in the approaching regime goes past the perception threshold it is referred to as the deceleration following regime. (PTV AG, 2011). The acceleration in the deceleration following regime is calculated using Equation 16.

$$b_{n+1} = 0.5 * \frac{\Delta x^2}{ABX - (\Delta x - L_n)} + b_n \quad (16)$$

$$b_{null} = -BNULLmult * (RND4_n + NRND) \quad (17)$$

The *"acceleration following regime occurs when a vehicle in the deceleration regime passes the opening difference in velocity threshold or a vehicle in the emergency regime passes the minimum following distance threshold"* (PTV AG, 2011). This regime is represented by Equation 17. When a vehicle in this regime crosses the following distance regime then it enters the free driving regime, vice-versa (Higgs, 2011). The emergency regime occurs when the space headway is below the minimum threshold. Equation 18 calculates the acceleration in the emergency regime (PTV AG, 2011).

$$b_{n+1} = 0.5 * \frac{\Delta v^2}{ABX-(\Delta x-L_n)} + b_n + b_{min} * \frac{ABX-(\Delta x-L_n)}{BX} \quad (18)$$

$$b_{min} = -BMIN_{add} - BMIN_{mult} * RND3_n + BMIN_{mult} * V_n \quad (19)$$

Where BMI_{nadd}, $BMIN_{mult}$ are calibration parameters and $RND3_n$ are normally distributed driver dependent parameters (Soria, 2010) (PTV AG, 2011).

In 1999, Wiedemann proposed another psychophysical model usually termed Wiedemann99 that is loosely based on the 1974 model. In the 1999 model, the thresholds are defined in a different way to model freeway traffic better (Gao, 2008). The threshold will not be discussed in this research.

2.4.4 Lane changing logic

Lane-changing characterizes the movement of vehicles from the subject lane to the adjacent lanes (Zhang, 2005). Though there are countless studies on car-following models, there is a gap in research on lane changing models due to the complexity of such models (Kusuma, 2015). Lane-changing models are considered complex because they have to include decision on which lane to move to and whether to accept available gaps. (Kusuma, 2015). According to its nature, lane changing is classified as either essential or non-essential. Lane change which is regarded as essential occurs when a vehicle changes lanes to maintain its path (e.g. exiting an on-ramp, merging with through traffic, at a lane area, avoiding a permanent obstruction). Lane changes which is non-essential refers to when a vehicle changes to avoid slow moving vehicles. The objectives of lane changing are to:

- avoid obstruction,
- accept a safe target gap,

- increase speed,
- move away from a heavy vehicle,
- avoid or move to a dedicated lane.

Lane changing is based on three steps that considers if it is necessary, possible and desirable to change lanes (Gao,2008). The three steps to lane changing is to derive the need to change lanes, to choose the target lane and accept an available gap. Necessity to change lanes is determined by the feasibility to overtake and the prevailing conditions in the primary lane. Desire to change lanes is based on foreseen improvements after lane changes. Possibility to change lanes is determined by the speed, queue length etc in the desired lane (Kusuma, 2015).

Over the years, research has resulted in different analysis methods that include fuzzy logic, game theory, gap acceptance and discrete choice methods amongst others. The basis of using this method, the theory behind them and the application of this methods in lane changing analysis are further discussed in the subsequent sections.

2.4.4.1 Decision making framework method

Rule based lane-changing models refers to models that follow a framework of rules that describe the procedures and processes included when changing lanes (Van Wageningen-Kessels *et al.* 2015). Decision based framework models take into consideration the necessity, desirability and safety of changing lanes. In his study, Gipps classified lane changing as either a discretionary or mandatory lane change. Discretionary lane changes depends on the safe an relative speeds between the primary and target lane and how close to collision the lead and target vehicles are (Gao, 2008; Kusuma, 2015).

The Wei *et al.* method was developed in 2000 (Kusuma, 2015; Wei *et al.*, 2000). The method is based on an empirical approach and identifies the movements of individual vehicles. The method classifies gap acceptance as the most crucial action. It is specified that all gaps need be accepted for lane changing to occur. The study indicated the duration for lane changing is affected by the vehicle speed where a slower moving vehicle requires a shorter duration to complete the movement (Kusuma, 2015; Wei *et al.*, 2000).

Most decision-making theories, (Balal *et al.*, 2014; Elefteriadou, 2014) express lane changing as a series of choices. The driver is continuously faced with binary choices; whether to change or to remain in the primary lane (Balal *et al.*, 2014). The selected choice is determined by the lane changing movement goal and the vehicle speed in both the primary lane and the target lane (Mu, 2013). Decision based lane changing models ignore

the heterogeneous nature of traffic and assume that the drivers are homogeneous because there is usually no difference in the response from different drivers when conditions are the same (Kusuma, 2015).

The shortcoming of these methods is that they don't consider the interaction between traffic and only look at vehicles as single entities. Lane changing in decision-based theory is determined by the goal of the lane-changing movement only. The model does not consider the speed of vehicles in the primary and target lanes. The goal in rule-based lane changing is usually predefined for a specific traffic condition. In reality, it is a result of a series of choices that are determined by the prevailing traffic in the current and target lanes. Some of these goals associated with the choices are essentially concealed from the driver and are only realized by the rest of the traffic streams. Because of these shortcomings, the rule-based lane changing models are unrealistic in representing the lane-changing algorithm.

2.4.4.2 Discrete choice models

The discrete choice model for lane changing is covered extensively by Yang and Koutsopoulos (1996), Ahmed *et al.* (1999) and Balal *et al.* (2014). In the models, lane changing is defined as a three-step process; to identify the need to change lanes, to choose the lane and to accept the available gap. The discrete choice models classified lane changing as being either mandatory or discretional. Mandatory lane change (MLC) is when a vehicle changes lane as a result of the prevailing traffic conditions, for example, to avoid an obstruction on the road. Discretionary lane changing (DLC) happens when the subject vehicle changes lanes to improve their driving condition, for example, a following driver might decide to change lanes with the aim of increasing its speed if the lead vehicle is slower. In both lane changing choices, the choice of the lane is related to the following criteria; the prevailing traffic conditions, the drivers desired speed, lane changing regulations, the available minimum acceptable gap, impatience factors and speed differentials (Kusuma, 2015).

The lane changing decision making process as proposed by Ahmed *et al.* (1999), and which is typical for discrete choice methods is demonstrated in Figure 2-4. The driver is faced with two decisions to either change lanes (MLC) or to remain in the subject lane and wait for a better acceptable gap $\overline{MLC}$. The driver will then evaluate the traffic condition of the neighbouring lanes to decide whether to perform a discretionary lane change at first attempt (DLC) or at a later stage $\overline{DLC}$. In most cases the driver selects the lane with better operational condition. After the driver has selected the desired lane, he will decide whether to accept or reject the available lead and lag gaps.

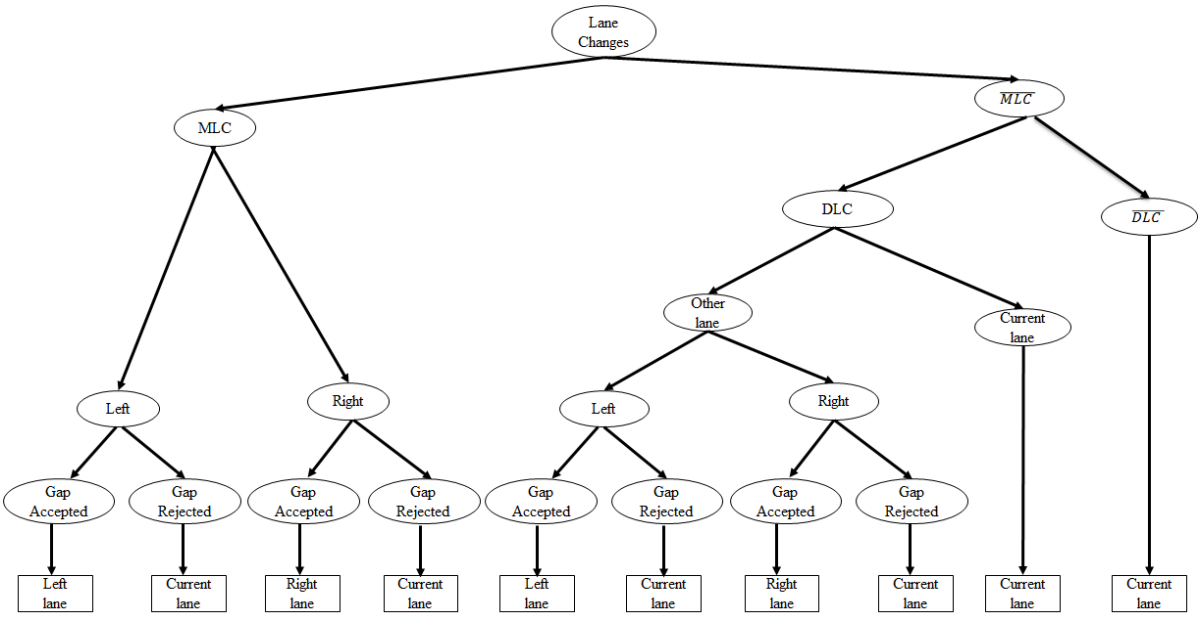

Figure 2-4: Lane changing decision making process, Ahmed *et al.* (1999)

This framework was refined by Toledo *et al.* (2005) to include a scenario where the choice lane is assumed to be all available lanes and not only the adjacent lane. The framework is depicted in Figure 2-5 below. The lane changing decision is a binary system consisting of lane acceptance and gap acceptance.

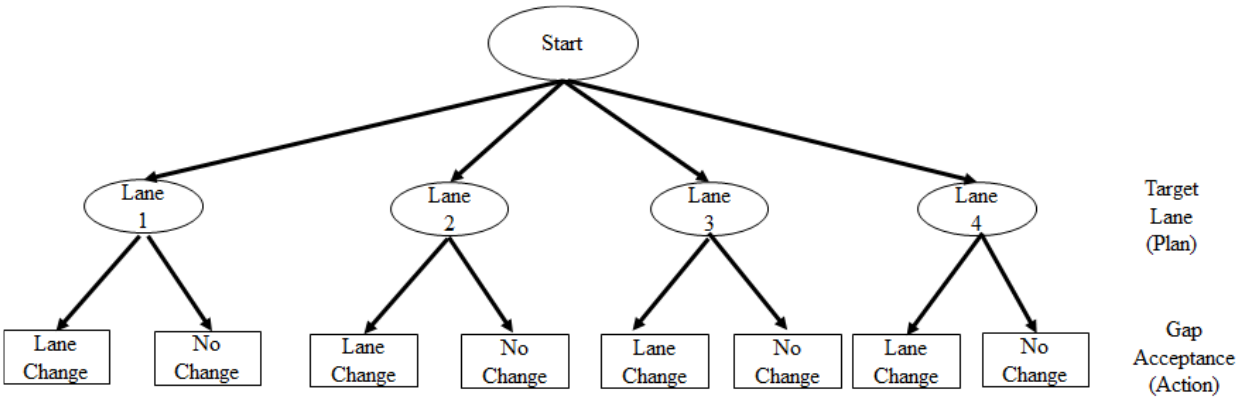

Figure 2-5: Binary isolated lane changing decision, Toledo *et al.* 2005

This model concentrates only on the isolated lane changes. The model is limited as it neglects the differences between group and individual lane changing which have significant effects on the weaving intensity and weaving section performance.

2.4.4.3 *Game Theory method*

The Game Theory method was introduced by Kita (1999) whereby lane changing is assessed as a "*two driver, non-zero sum, non-cooperative*" game (Kita, 1999). The model was developed to define the traffic behaviour and interaction of a pair of merging and through vehicles. The vehicles will take the optimal actions through forecasting the action of the other vehicle. For example, a merging vehicle may decide to merge into the through lane following a speculation that the through vehicle will slow down or change lanes (give away). The noticeable limitation of this model is that it only considers the neighbouring vehicle's position and speed as a determinant of the lane-changing outcome. In reality, the decision as to whether or not to change the lane is determined by the traffic conditions in wider area.

Other notable contributions to the Game Theory model in lane changing are by Wang *et al.* (2014). The models introduced in these studies are derived from decision-based lane changing. The models assume that the driver in the primary lane will control their speed, with the aim of maximizing the possibility of available gaps while considering both the neighbouring traffic and the distance to the lane-changing location. The model is an integration of the acceleration, gap acceptance, merge and cooperative models. The cooperative model relates to the cooperation between traffic and the subject vehicle. For instance, traffic conditions and behaviour will affect the ability of the lag vehicle to create gaps, hence allowing the lane-changing manoeuvre (Kusuma, 2015). The game operates by allowing the neighbouring vehicle to accept the first gap, while the subject vehicle accepts the second or following gaps. This model indicates the dynamic interaction of vehicles during lane-changing manoeuvres.

Game Theory models were further improved by Liu *et al.* (2007), in which it was assumed that the sub-aim of the subject vehicle is to maintain the overall traffic conditions. In the game, the subject vehicle strategy is to overtake and look for the next available gap or change lanes, as vehicle in the target lane strategy is to slow down in order to give way or maintain the speed. The game follows the framework proposed by Kita (1999) by analysing the game as dual-player game between the subject vehicle and the lead vehicle (Higgs, 2011). The difference of the former research is that these models acknowledge that the forcefulness of the subject vehicle intensifies when the lead vehicle decides refuses to give way. A deceleration movement by the subject vehicle would allow the lag vehicle to move comfortably. Though these models have similar shortcomings as the theory proposed by Kita (1999), in that they concentrate only on the neighbouring conditions, it should be noted that neighbouring conditions are partly a reflection of the traffic both upstream and downstream.

2.5 Historical overview of analysis methods

2.5.1 Macroscopic models

Analysis of weaving sections dates from the Highway Capacity Manual (HCM) of 1950 (HCM, 1950). Since then new approaches and updates to analysis methods have been developed. This section of the literature review seeks to study the methods produced over time to analyse weaving sections.

The data used in the HCM's 1950 edition (HCM, 1950) was based on field data collected in 1947 in the United States, (Washington D.C. and Virginia), (Jack. E. Leisch & Associates, 1984). The method emphasized capacity and operational speeds on freeways with weaving sections (Zhang, 2005). Various definitions were provided in the manual and research findings stated. One finding relevant to our study was that if all vehicles were to perform a weaving manoeuvre simultaneously, the number of vehicles passing through the weaving section should not exceed the capacity of a single lane (Richard *et al.*, 2001).

Research in years succeeding the HCM (1950) expanded on the methodologies and findings of the manual. This research was adopted in HCM (1965). The manual added flow quality in the analysis (Zhang, 2005). It graphically depicted the relationship between weaving length and volume, and quality of service (Skabardonis and Kim, 2010) (Richard *et al.*, 2001).

More research uncovered inaccuracies in HCM (1965) even though it noted much improvement from the earlier edition. The inaccuracies were ascribed to not including lane and road configurations as a parameter in the analysis method (Richard *et al.*, 2001). They found that weaving movement in weaving sections takes place in shoulder and auxiliary lanes. The National Cooperative Highway Research Program (NCHRP) report 159 in 1975 (cited in Richard *et al.* 2001) found that Level of Service (LOS) and flow quality are not dependent upon each other and that geometric configurations play a crucial part in the weaving section capacity. It was also found that the LOS in HCM (1965) tends to be higher than actual operational conditions.

Leish in his 1981 study (cited in Skabardonis and Kim, 2010) proposed a new procedure for analysing weaving sections. The procedure was presented in nomograph similar to the approach in HCM (1965), with the difference that two graphs were presented, one for one-sided and the other for two-sided weaving areas. The nomograph output included the LOS of the weaving area, the number of lane required to reach a certain LOS. The method was found to be easy to apply, however some demerits of the method were found such as that the procedure fails to predict the speed of the non-weaving traffic. The method was found to yield results that were substantially different to those of other methods. The monographs were calibrated based on experience and limited data.

A study was commissioned in 1984 by the Federal Highway Administration (FHWA) with the aim of consolidating the different methods into one procedure. Methods preceding this period were found to be inadequate for analysing the freeway weaving section. Consequently, a new procedure, termed the JHK method was proposed to analyse weaving sections (Reilly *et al.*, 1984). The procedure was based on two equations that predicted the speed of both weaving and non-weaving vehicles and a graph from which weaving and non-weaving LOS can be read out.

The outcome of the study formed the basis of the updated HCM published in 1985 (HCM, 1985). The manual was based on a refinement of the JHK method using 15 min window calibration parameters for both constraint and unconstrained operation of weaving and non-weaving traffic (Zhang, 2005). It was established through the output of the model that the weaving capacity is 1800pcph for type A configurations and 3000pcph for type B and C configurations (Zhang, 2005). The road configurations are discussed in Section 2.1 above.

In the few years following the publication of HCM (1985), Fazio (cited in Zhang, 2005) conducted a study with the aim of comparing and refining the Leisch, HCM (1985) and JHK methods. The study looked at the required inputs, performance and limitations of the methods. The refinements included accounting for traffic upstream and lane shifts within weaving segments. The authors found that by including the lane shifts and by accounting for traffic upstream of the weaving section, more accurate depictions of speed were attained. These speeds were more accurate than those predicted by the three methods

Skabardonis *et al.* (1989) undertook a study of freeway weaving sections in which results from the simulation software INTRAS, a microscopic model, were compared with field measurements. The study concentrated on eight sites with differing weaving and lane configurations. The findings indicated that the INTRAS model yielded results, which were representative of the traffic operation on all the eight sides. Through this study, it was determined that there is a slight variance in speed and there is instance of increased traffic volume under moderate flow. Further to their core objective, they analysed the factors that most influence the weaving operation. Concerning this, it was found that speed is not necessarily a good measure of effectiveness for a weaving section but that operations are based on actions within individual lanes.

The highway capacity manual was refined in 2000 (HCM, 2000). The refinement included some research findings from work done between 1985 and 2000. Traffic LOS for weaving and non-weaving sections was estimated based on the average density of vehicles in the steam. In the same year of the publication of HCM (2000), Kwon *et al.* (2000) conducted a study in which an online method was proposed for estimating the capacities of weaving

sections. The finding of the studies suggested that the geometric configuration of the exit ramp affects the speed of the exiting traffic, under free flow conditions. One finding of the study was that as the volume of the weaving vehicles increases, vehicles exiting the highway are prone to change lanes earlier within the weaving section. It was also noted that the vehicles entering the freeway are prone to driving on the auxiliary lane before entering the mainstream.

After HCM (2000), research was focused on different approaches to analysing weaving sections. Most methodologies veered from analysis based on speed and looked into other methods such as lane-changing models (Wang *et al.*, 2014) and point flow approaches (Ostrom *et al.*, 1993). These methods will not be discussed at depth as the data available for the proposed study only allows for analysis using speed prediction methods.

In 2010, the HCM was further refined (HCM, 2010). The governing principle remained the same as with the manual published in 2000. However, definitions such as weaving length and configurations were changed to account for a wider range of designs. The manual stated that the main geometric factors that affect the weaving sections are length, width and configurations of the weaving section,. The noted improvement of the manual is that it provides wider definitions that are inclusive of different road designs.

2.5.2 Microscopic models

2.5.2.1 INTEGRATION

INTEGRATION is a trip based microscopic simulation model developed in 1983 by Michael Van Aerde (Gao, 2008) The model provides an integration of freeways and arterials and can perform microsimulation and traffic assignment in the same model. The model provides data on detailed driver behaviour and traces individual vehicle trajectories with a high level of resolution. Like most microsimulation models, the model computes car emissions, delays and vehicle speeds.

The car-following logic in INTEGRATION combines two car following models, ie. Pipes and Greenshields. The combination overcomes the shortcoming of these models, especially the shortfall in the Pipes Model, that assumes that speed and flow have a parabolic relationship (Rakha and Crowther, 2002). The INTEGRATION lane-changing model considers both discretional and mandatory lane changing. Discretionary lane changes are modelled by computing the speed at which a vehicle will/or may maintain in the primary lane and the speed that the vehicle may adopt when changing lanes to the neighbouring lane which is based on the available headway.

The prerequisite of performing a lane change discretionary is that there must be available an adequate gap in the neighbouring lane (Gao, 2008). Once a discretionary lane change has been made, the mandatory lane change becomes a principal.

2.5.2.2 CORSIM

Corridor Simulation model, also known as CORSIM, was developed in 1996 by the FHWA (Halati, et al., 1997) . It is also a microscopic simulation model that models corridors, freeways and urban streets. The model was developed from FRESIM which models uninterrupted facilities and NETSIM that models arterials (Bloomberg & Dale, 2000).

The car-following model in CORSIM looks at the speed differential between the leading vehicle and the subject vehicle, together with the distance headway. (Rakha and Crowther, 2003). The model adopts the logic that the subject vehicle will move to a position at which the deceleration of the leading vehicle will have no impact on the reaction time and braking ability of the subject vehicle such that the subject vehicle can come to a stop without creating a collision. The lane-changing logic in CORSIM is based on Gipps decision model (Gipps, 1986). The logic looks at both the mandatory and discretionary lane changes.

2.5.2.3 PTV VISSIM

PTV VISSIM is microscopic traffic simulation software that is behaviour based and follows time-steps (PTV AG, 2011). The software simulates public transit operations and urban traffic and computes the measures of effectiveness, such as delays. It can also include different vehicle types under different traffic control situations.

The car-following model in PTV VISSIM is a psychophysical model that defines driver perception thresholds, that was developed by Wiedemann for freeway traffic, arterials and corridors (PTV VIsion, 2011). The lane-changing logic was developed by Willmann and Sparmann (Gao, 2008). In the model, lane changing can be either towards a slow or a fast neighbouring lane. For lane changing to occur, three conditions need be held, i.e. the desire to change lane, the condition in the desired neighbouring must be desirable and the movement must be possible. Lane changing in this model is classified as being either free lane changes or necessary lane changes. Necessary lane changes occur when a vehicle needs to connect to the next route, and free lane changes occur when vehicles

require faster speeds. Regardless of the type of lane change a desirable gap must be present for any lane changing to occur in this model.

2.6 Conclusion

The aim of this review was to get an understanding of the history of the analysis of weaving sections. The literature indicated that earlier methods had shortcomings and mostly yielded inconsistent results. No empirical data was used to validate the methods. A number of these methods were founded on insufficient data that does not account for varying geometries and configurations. A summary of the methods through the years is shown overleaf.

A lot of research went into the development of the HCM, and new developments are included in the latest editions. For this reason, the analysis tool that is proposed to be used on this project will be the method in the HCM published in 2010 (HCM 2010). The manual was found to be user-friendly and incorporates work of several independent researchers done since the year 2000 edition and prior to the 2010 edition. For this reason, the microscopic model that will be used for analysis is PTV VISSIM as recommended in HCM (2010).

3 PROPOSED CASE STUDY

A site that experiences problems regarding vehicle weaving within the road segment was identified as a case study for this project. The site experiences different problems regarding vehicles weaving because of the geometric layout of the road or due to illegal manoeuvres carried out by drivers and it also does not follow a typical weaving segment description as provided in HCM (2010). This chapter provides a description of the case study site and the geometric properties of the site.

3.1 Location

The case study, as seen in Figure 3-1 is identified as the section of the N1 freeway between the R300 and Okavango Road Outbound. This includes the two on-ramps and the one off-ramp. The site is located within City of Cape Town in the Western Cape Province of South Africa and falls within the jurisdiction of the South African National Roads Agency (SANRAL).

3.2 Description

The case study focuses on the outbound carriageway of the N1 (heading north-east) for a distance of 2.6 km in Western Cape. The segment is bounded by the entry on-ramp at the R300 (referred to as access point (OR1)) and the off-ramp to Okavango Road close to the Cape Gate mall (FR1), as depicted in Figure 3-1 below. The case study incorporates one other on-ramp from Brackenfell Boulevard (OR2) downstream of OR1. This section of the N1 is a two-lane dual carriageway with 3.7 m lane widths. The ramps consist of a single lane of 3.7 m width. The R300 on-ramp comprises two lanes which are merged into one lane approximately 250 m before the merge point with the N1. The Okavango Road off-ramp is a single lane diverging from the N1, and splits into two lanes 250 m after the divergence point. There is no auxiliary lane connecting the on-ramps and the off-ramp, therefore the weaving behaviour noticed at this section is not a result of the Type A weaving geometric layout as per the conventional description.

The distances from the R300 (OR1) to Brackenfell Boulevard (OR2) and Okavango Road (FR1) are as follows:

- OR1 to OR2 : 990 m
- OR2 to FR1 : 1160 m

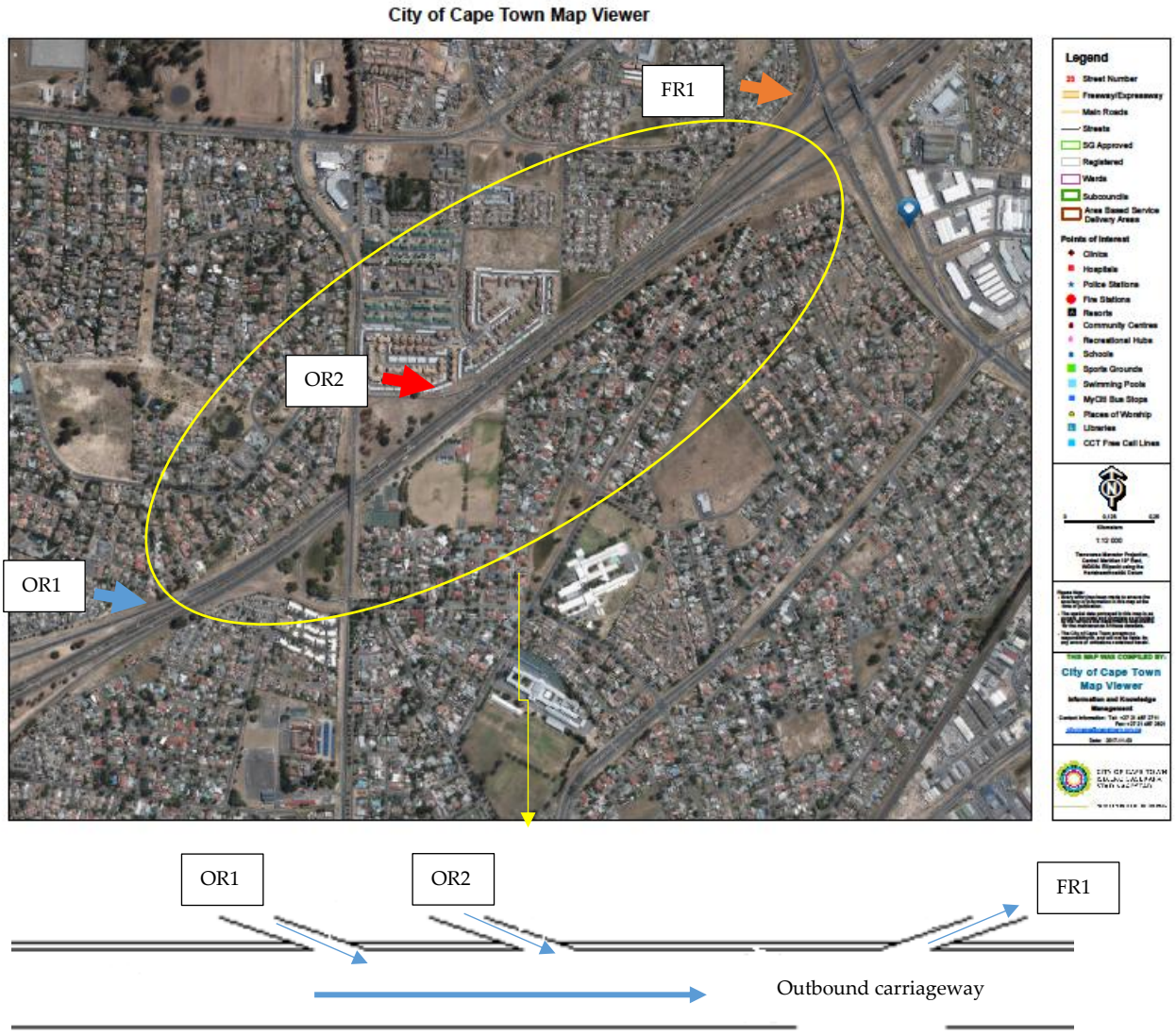

Figure 3-1: N1 Between R300 and Okavango Road

4 PROPOSED METHODOLOGY

4.1 Overview

The research aimed to, aided by a case study, assess the characteristics of unconventional weaving traffic within freeway sections that result from operational constraints, thereby gaining a more detailed understanding of unconventional weaving behaviour, causes and possible solutions. Unconventional weaving refers in this report to weaving that does not conform to the conventional definition of a weaving manoeuvre as per HCM (2010). The research is based on a case study area identified in Chapter 3. The methodology that will be followed in achieving the research aim is summarized below and detailed in the following Sections. The steps are:

- Step 1: Identify an area presenting unconventional weaving within the Western Cape Province
- Step 2: Collect traffic data using both video recordings (CCTV) and roadside sensors and information relating to the design of the selected study area
- Step 3: Perform simulations of the traffic within the study areas using PTV VISSIM to understand traffic behaviour within the study areas, analyse the weaving data and study the relationship amongst traffic fundamental properties in the areas
- Step 4: Propose general solutions to the problem and where possible, simulate the effects of the solutions

4.2 Step 1: Identify the case studies

The research case study that was mentioned in Chapter 3 was selected with the help of and through consultation with SANRAL. SANRAL had identified areas where there where high accident zones and points of conflict between vehicles that could be attributed to weaving movements. The proposed case study is a section that has displayed high numbers of weaving movements and significant safety concerns.

4.3 Step 2: Data collection

4.3.1 Background of data collection

The data used for this research was made available to the student by the SANRAL Western Region through their existing partnership with the Stellenbosch Smart Mobility Lab (SSML) of the University of Stellenbosch. The data collection process, background and description are discussed in this section.

4.3.2 Description of the data

Two data sources were used towards achieving the research objectives. Data was collected from Vehicle Detection System (VDS) radar devices and CCTV cameras located at numerous positions along the Freeways of Cape Town as part of the Cape Town Freeway Management System. VDSs and CCTV cameras (cameras 118N1, 119N1 and 120N1) along the Case Study route segment were chosen.

The VDS data on the N1 was obtained from DS VDS 118 OB and DS VDS 119 OB on the N1 outbound and DS VDS 314 North on the R300.

Geometric data was based on Google Maps and the City of Cape Town's Map Viewer (https://citymaps.capetown.gov.za/EGISViewer/). No as-built drawings were available for research purposes. The information on the map was clear and contained comprehensive information required for the purposes of this research.

Traffic recordings were reviewed to understand the interaction of traffic and to see actual weaving behavior on the selected sections of road. Recording were reviewed from CCTV cameras 118N1 and 120N1 for the following date:

- 7 July 2017 N1 OB (PM)

Where N1 OB refers to the National Road 1 outbound direction.

The weather on the date of recording was clear.

4.4 Step 3: Overview of the data analysis program and calibration process

The simulation software used in the analysis is PTV VISSIM (refer Section 2.5.2.3). The software was chosen for the following reasons:

- It is behaviour-based
- It follows time steps
- It is microscopic, and
- It can model a freeway and an arterial simultaneously

4.4.1 Calibration procedure

A systematic calibration process was followed in ensuring that the outputs of the PTV VISSIM model are representative of the actual site environment. The calibration procedure was based on the process used and documented by the Virginia Transport Research Council (Park & Won, 2006), as depicted in Figure 4-1 and further discussed in the following sections.

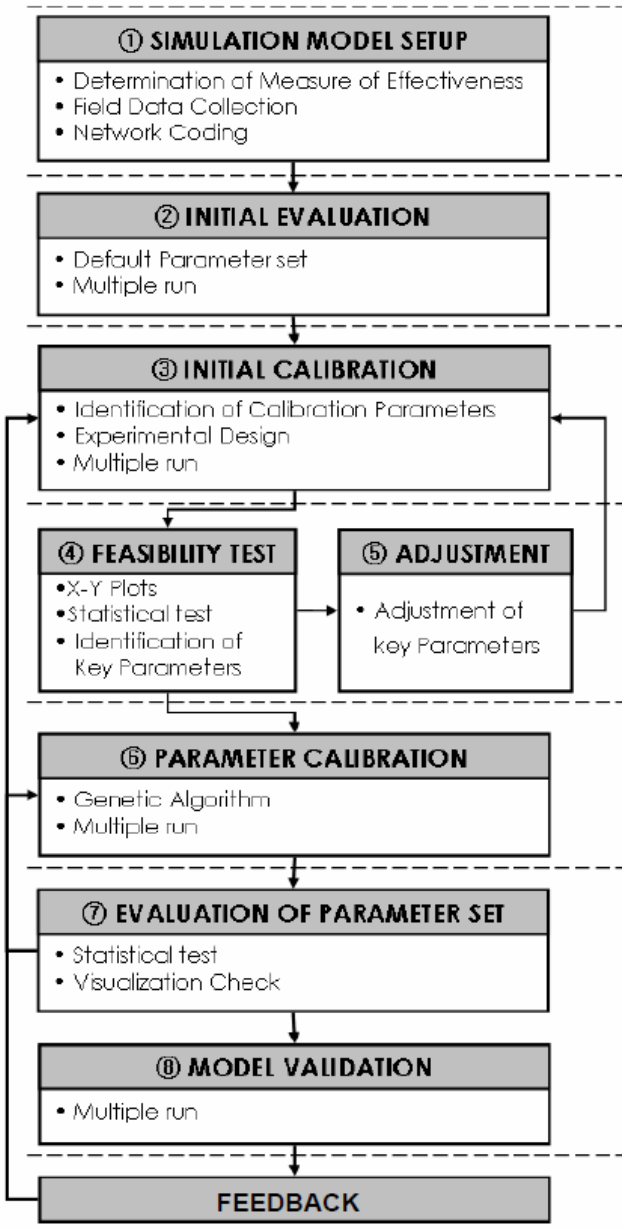

Figure 4-1: Proposed Calibration Procedure (Source: Park & Won, 2006)

4.4.2 Feasibility of default parameter set

The feasibility of the default parameter set has to be established as the initial step towards calibration. The feasibility test follows two steps; running the simulation with the default parameters followed by verifying the output through comparison with the data collected from the field devices. Multiple runs of varying seed values will be run with the default parameters. The output of the multiple runs will have a certain distribution and will be represented through a histogram. The validity of the default parameters will be verified by using a histogram. Feasibility is examined by comparing the histogram resulting from the multiple runs and field data collection. Parameters are feasible when all field data sets

fit inside the distribution depicted as a histogram. However, when not all datasets fit within the histogram, the initial parameters are not feasible, and a check of the calibration parameters range has to be performed (Park & Won, 2006).

4.4.3 Range check of each calibration parameter

The next calibration procedure is to check the parameter range. This is done by selecting parameters that influence the results. A range for each parameter will be set based on experience, available data and compatibility. This is followed by a check to see whether the parameters are reasonable. This is done by performing multiple runs with a combination of various parameters. As the combination of multiple parameters and their ranges is enormous, sampling of a possible parameter set is advised. This can be done by using the Latin Hypercube Design, which is recommended by Park & Won to decrease the number of parameter combinations to manageable size. After multiple runs, the next step is to verify the feasibility of the calibration range. The results of the multiple runs can be presented in a histogram. A parameter range check is performed to see if the field values fall within the middle 90% of the distribution, as specified by Park & Won(Park & Won, 2006).

4.4.4 Adjustment of parameter range

In a case where no parameter set is acceptable, further analysis of the parameter range is required to find an acceptable set that will be used for the main calibration process. The parameter feasibility is checked by using the X-Y plot, which provides a two-dimensional histogram. Its main purpose is to discover the relationship between variables. Key parameters are observed by checking the X-Y plot of each calibration parameter. In cases where a clear relationship is observed, the parameter may be taken as a calibration parameter. In the case of a scattered graph the parameter will be regarded as not being feasible and can be ignored during adjustment as it does not significantly affect the model output (Park & Won, 2006).

4.4.5 Finding the optimized parameter set with selected ranges

After determining the range of the calibration parameters, a specific set of parameters that reproduces field data needs to be determined. This is done by using the General Algorithm (GA) (Park & Won, 2006). The GA performs evaluation of a chromosome through the fitness function. After the formulation of the fitness function, a fitness value is determined. The chromosome is defined as parameters that provide a proposed solution that we are trying to solve using the GA. The GA formula calculates the ratio of the parameter value obtained from the field data and that from the simulation. In a case where the results are unacceptable, the GA process has to be repeated with the current chromosome as a starting point. If a fitness value is less than predetermined criteria the results are deemed acceptable. The GA tries to find a calibration parameter that

reproduces field conditions by performing multiple simulations generations. As the generation number increases, a more accurate parameter set is found that reproduces field conditions Park & Won, 2006).

4.4.6 Evaluating and validating a calibrated parameter set

The first step in evaluating the results is to compare the default and calibrated parameter set. This is done by checking whether the calibrated parameters reproduce field conditions within an acceptable range. The performance is compared by using a histogram or a line chart that was used previously in the initial run with default parameters to check acceptability of the model (Park & Won, 2006). The measured field data must fall within the range of the histogram and the line chart to conclude that the calibrated model performs better than the default one.

The other evaluation check is the visualization of the model, to check for any unrealistic vehicle movements. This is done by checking the animation of the simulation model that was ran with random seeds that would produce output at different intervals.

The last step of the simulation is to validate with unused data, which if successful indicates that the model with the calibrated parameters set is valid for different cases. This is done by performing new multiple simulations with the unused data with different seeded numbers. The simulation output is then presented in a histogram. If the field measured parameters fall within an acceptable region of the histogram, then it can be concluded that the model has been calibrated and validate. The acceptable range is within 90% confidence (Park & Won, 2006).

5 MODEL DEVELOPMENT

As mentioned in Chapter 4, the simulation software used for data analysis is PTV VISSIM version 9. A model was created for the case study area. The inputs required for setting up the model include geometric data, traffic flow data and driver behaviour information.

5.1 Geometric data

The inbuilt aerial map in PTV VISSIM was used to visualize the study areas. The road network relevant to the case study was traced over the map. Network geometric properties such as the number of lanes, lane widths, positions of the merging and diverging lanes and posted speed limits were incorporated into the network to better visualize the existing conditions. The geometric information used was based on high resolution scaled aerial photographs of the City of Cape Town road network Map Viewer. The information extracted from the aerial maps included the lane configuration, road markings and the horizontal alignment. This data was mostly verified based on field investigations.

Roads segments in PTV VISSIM are referred to as links. Links are defined as having constant properties such as the number of lanes and traffic. To create an entire road network, multiple links with varying properties were created. Links were also classified based on the driving behaviour within the roadway. For the case study, the links on the freeway were classified as such and those on the ramps as urban streets.

Figure 5-1: Aerial representation of the section of N1 under consideration

Figure 5-1 provides the layout used for the case study. The case study was modelled with two lanes each of 3.7 m width on the freeway and lane widths of 3.7 m on the ramps. The section of road is relatively straight with no sharp curves.

5.2 Traffic flow data

Vehicle classification

Traffic flow data used in the models was based on vehicle counts for 14 July 2017 that was obtained from SANRAL Western Region. The counts included vehicle classification, vehicle volumes and speeds. Vehicles were classified based on performance characteristics and driving behaviour. The default vehicle classifications used in PTV VISSIM and adopted in the case studies are Car, High Occupancy Vehicles (HOV) (buses and taxis) and Heavy Goods Vehicles (HGV) (Heavy trucks). Vehicles with the same classification share attributes such as the width, length, weight, maximum acceleration and occupancy.

Vehicle distribution

The mix and distribution of vehicle types are referred to as traffic composition. Traffic composition is considered one of the vehicle input sources and is entered at the source nodes. For the case study, the N1 (south end of the model) and the R300 on-ramp and the on-ramp at Brackenfell Boulevard were defined as source nodes. It was assumed that the traffic composition on the freeway could be approximated by the composition on the ramps.

Traffic Volume

Traffic volumes in PTV VISSIM are assigned at origins, which are also referred to as routing decision points. A route is a fixed continuous combination of links and connectors from an origin to a defined destination or destinations. To realistically represent the field condition, it was ensured that balanced volumes and flows were entered throughout the route for each model.

For all the models, the traffic volume used in the analysis was based on the highest average daily traffic (ADT) recorded over the three days on the freeway. The date corresponding to the highest ADT was selected at the model day. For the case study, the N1 link, the volume therefore represents the traffic of the 14 July 2017 as recorded by VDS 118. The volume was selected as exact in the PTV VISSIM simulation.

Travel speed

Travel speeds in PTV VISSIM were defined as a distribution, based on the VDS data, to realistically represent traffic along a network. The defined distribution influences the capacity of the link and the achievable speed. The posted speed limits for the case studies and VDS measurements were used to define the distributions. Speed distribution was modelled which represents changes in speed resulting from the geometric conditions especially at on-ramps were vehicles enter the main freeway. The graph below shows the speed distribution used in the simulation for Case Study 1, 85th percentile of 103.5 km/h, 15th percentile of 81.8 km/h and 30th percentile of 88.2 km/h.

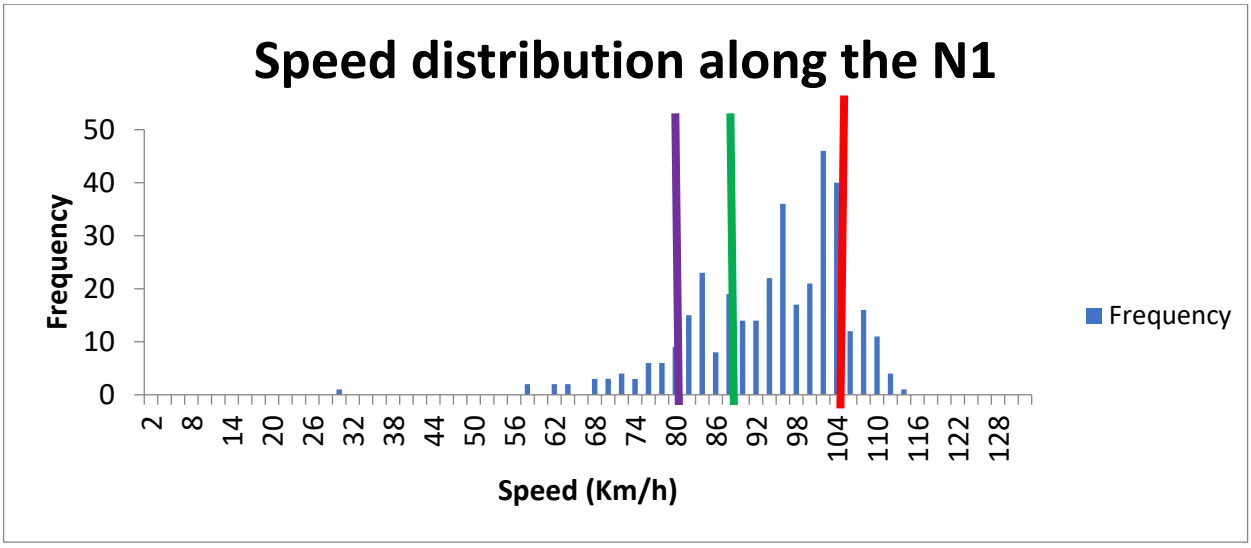

Figure 5-2: Speed distribution on the N1 as applied in the case study

5.3 Summary of data used

Table 5-1 provides a summary of the data that was provided by SANRAL Western Region for purposes of conducting this study. The table indicates the average daily traffic (ADT) and the percentage heavy vehicles on the N1 (based on VDS 188) and on the R300 (based on VDS 314) over a period of five days from 10 July to 14 July 2017. The highest ADT was adopted for modelling purposes.

Table 5-1: Traffic Counts on the Section of N1 under Consideration

Date	N1 (VDS 118)		R300 (VDS 314)	
	ADT (Veh/d)	HV (%)	ADT (Veh/d)	HV (%)
10 July 2017	26 407	4,2	13 309	5,3%
11 July 2017	26 361	3,8	13 350	4,5%

Date	N1 (VDS 118)		R300 (VDS 314)	
	ADT (Veh/d)	HV (%)	ADT (Veh/d)	HV (%)
12 July 2017	26 648	4,4	13 859	4,7%
13 July 2017	27 919	3,8	14 352	4,3%
14 July 2017	**28 987**	**3,8**	**14 772**	**4,7%**

6 MODEL CALIBRATION AND VALIDATION

6.1 Identification of calibration parameters

PTV VISSIM provides two types of driving behaviour models: the Wiedemann 94 and Wiedemann 99. The Wiedemann 99 model is considered to be an appropriate model for freeways and was therefore selected for the case study. 10 calibration parameters related to lane changing and car-following behaviour were selected. The following is the first set of parameters that was selected for calibration purposes (PTV AG, 2011).:

Table 6-1: Identified initial parameter set for calibration

Parameter Description (units)	Default	Proposed range
Simulation Resolution (time steps/s)	1	1 to 3
Number of observed preceding vehicles	1	1 to 4
look back distance (m)	200	100 to 300
Emergency stop distance (m)	5	1 to 5
Waiting time before diffusion (s)	60	20 to 80
Standstill distance: CC0 (m)	1,5	0,5 to 2
Headway time: CC1 (s)	0	0 to 30
Following threshold: CC4	0,35	0,1 to 0,5
Safety distance reduction factor	0,6	-

6.2 Initial runs with default parameters

The second step followed in calibrating was to determine the required number of model runs such that the model output will provide a fair representation of the field conditions at a reasonable confidence level. The following procedure was used to calculate the required number of runs:

- Six initial simulation runs were performed with the default parameters
- The standard deviation of the results of the six runs was determined for each hour
- A result confidence level of 90% was selected

- The number of minimum required repetitions was calculated as the ratio of the confidence level combined with the T statistic and the standard deviation.

The minimum required repetition was found to be six. The results from the initial six simulations were taken for further evaluation. All simulations performed for purposes of this study were repeated six times with differing seed values.

6.3 Feasibility test with default values

The results from the initial six simulations were analysed to assess whether the default parameter sets were valid for the case studies. The validity of the default parameter was assessed and verified through statistical and graphical methods. A histogram analysis was used. The histogram provides a number of data points that fall within a certain interval. In the case study the histogram represented the distribution of frequencies of discrete variables (which, for this case study, were the simulated flow results). For purposes of comparison the simulated dataset and traffic flow were analysed against the collected field dataset. Validity was further checked by plotting a scatter graphs of collected field data (traffic flow) and assessing whether the collected flow rates fit within the histogram distribution range of the simulated flows. The defaults parameters are deemed to be valid when more than 90% of collected datasets fit inside the distribution of the simulated flow. Figure 6-1 provides the results of the histogram analysis for the case study.

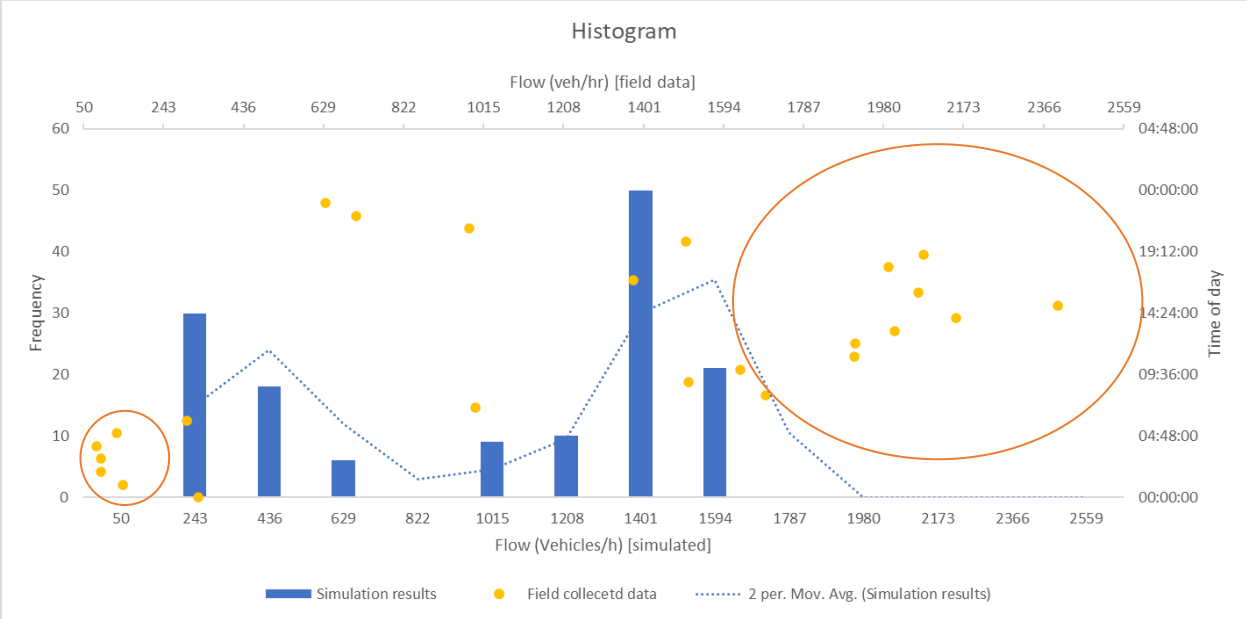

Figure 6-1: Feasibility test results based on default parameters

Figure 6-1 shows a histogram with primary axis (traffic flow rate and frequency) been of the simulated dataset and the secondary axis (traffic flow rate and time) belonging to the filed collected dataset. The figure shows that most flow rates (which are circled in red) of the field data are either lower or higher than the simulation outputs and fall outsides the distribution range. This shows that the default parameters do not fully represent field conditions and therefore require adjustment. The flow histogram shows that more than 90% of the field volume data falls outside the simulation volume distribution. It can therefore be concluded that the parameter sets were unable to reproduce the field condition and cannot be used for further calibration purpose.

6.4 Experimental design and feasibility test for calibration

X-Y scatter graphs, shown in Figure 6-2 were plotted to further determine the parameters that show a relationship with the volume output. The following parameters indicated a strong relation with the volume output when compared with other parameters:

- CC1 (Headway Time)
- CC4
- Simulation resolution

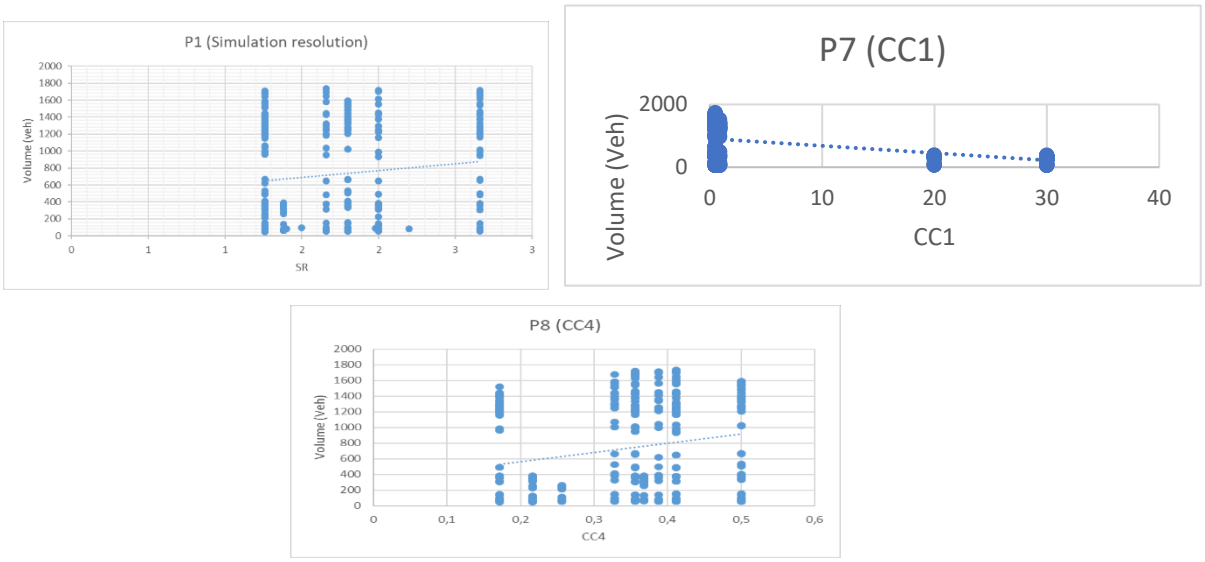

Figure 6-2: Key calibration parameters

A feasibility test was conducted to assess whether the field collected data fits within the distribution of the simulated flow rates based on the calibration parameters. The feasibility test also checked whether the output could estimate key calibration parameters. Figure 6-3 indicates a shift to both the left and right of the simulation flow rate distribution range with the selected calibration parameters to accommodate lower and higher field flow rates. It also shows that three

(circled in red) out of the 24 field collection data slightly falls outside the simulated flow rate. The model and its parameters are therefore deemed calibrated and falls within 90% confidence level. As seen on Figure 6-3 the field collected data in orange fits within the distribution range of the calibrated simulation flow rate results.

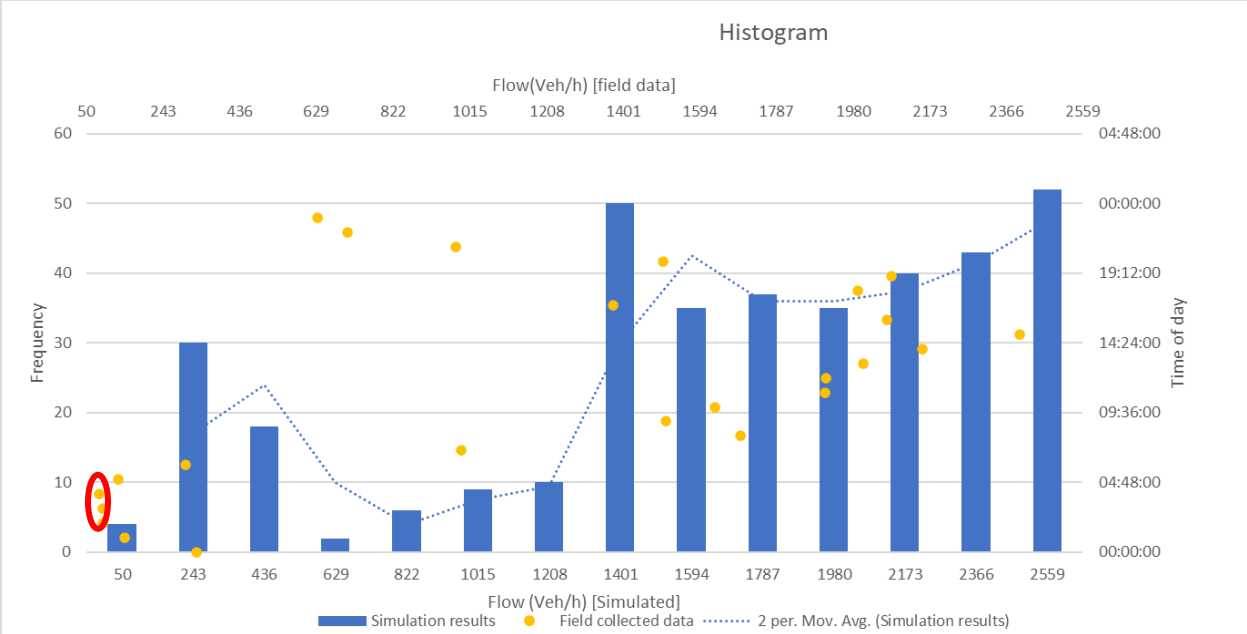

Figure 6-3: Feasibility test results based on calibration parameters

6.5 Evaluation of parameter set

To evaluate parameters, the list of default parameters and calibrated parameters is tabulated in Table 6-2. The model based on the default parameter sets produces output flow rates with mixed distribution with some values lower than field (measured) flow rates and some higher than the field flow rates. The calibrated model is 15% within the average field flow rates.

Table 6-2: Calibrated parameters and default parameter sets

Parameter Description	Calibrated	Proposed range	Default
Simulation Resolution	10	1 to 3	1
CC1	0.5		
CC4	-0.35	0,1 to 0,5	0,35
Minimum Gap	5	3 to 6	5

The distribution of volume from calibrated parameter showed narrow variation when compared to field (measured) volumes. Animations of the calibrated PTV VISSIM model were viewed and deemed acceptable and congruent to field video recordings.

6.6 Model validation

The model was validated by using traffic flow data from a different day, the calibration data from the previous chapters and fundamental traffic data to reinforce the viability of the calibration parameters. The data used for validation is from the 11 July 2017. The field data was then compared with the distribution resulting from the validation model. The data was found to be within the distribution range, furthermore, supporting the viability of the calibration parameters.

7 OPERATIONAL REVIEW OF THE CASE STUDY ROAD SEGMENT

7.1 Traffic flow behaviour in and around the weaving section

7.1.1 Lane-Change Manoeuvres

Lane changes were assessed from a running PTV VISSIM model and from the video recordings. The PTV VISSIM model indicate that there is a variance in lane changing patterns and their rates along the stretch of the road. Based on these results, it can be reasoned that the presence of two on-ramps and one off-ramp within the case study and in short succession of each other , affects the lane changing behavior along the road and especially at the moment when traffic exists off to Okavango Boulevard off-ramp. This is because a high number of vehicles on the road exit the freeway at the Okavango Boulevard off-ramp.

Lane changes over the length of the case study were observed when the model was running. Lane changes are prominent in the morning peak hours between the hours of five and eight and also in the evening peak, when volumes are the highest. The high rate of lane changes is indicative of a relatively high freedom of movement and increased headway for the morning peak. Vehicles have more chance to change lanes and to weave in the morning peak. The rate of lane change remains relatively constants between eight hours and the evening peak. For the evening peak, the high lane changes are a result of high volumes and flow on the road. The rate of lane changes can therefore also be correlated with the volume on the road.

7.1.2 Bottlenecks

Traffic bottlenecks were assessed when the model was running and by presenting results, in order to understand the nature of congestion experienced on the road. Traffic bottlenecks were taken to refer to constriction and/or disruption of traffic movement due to a physical condition which in the study case refers to the design of the road. Bottlenecks were assessed using delays and lost travel time. For purposes of analysis and in line with PTV VISSIM, delays refer to additional travel time that a vehicle experience (HCM, 2000). This refers to the difference in the ideal measured travel time during off-peak and the peak travel time. It is, therefore, the percentage by which travel time is more than the ideal off-peak time.

Densities and delays were analysed in PTV VISSIM to assess any bottleneck formations resulting from them. Figure 7-1 provides a delay heatmap for the case study to indicate

arears with recorded high and low delays. The Figure shows that there are generally moderate to high delays encountered on the N1 of between 35% and 40% (Orange) more than the ideal off-peak travel time. These delays are from the start of the project on the N1 and through to the Okavango Boulevard off-ramp. The delays are a result of dissipation of queues that is interrupted by the formation of a new queue at the on-ramps.

Delays are the longest on the R300 on-ramp and the 100 m section where the Brackenfell Boulevard on-ramp connects to the N1. These areas of high delays are depicted in white on Figure 7-1 and represent delays higher than 50%. The off-ramp at the Okavango Boulevards also shows high delays of between 45% and 50% (red). Bottleneck formation is evident at three locations, i.e. the R300 on-ramp, the Brackenfell Boulevard on-ramp and the Okavango Boulevard off-ramp. The long delays on two on-ramps result from drivers waiting for a feasible acceptable gap to merge to the N1 traffic. It would normally take some time to accept the gap as the traffic on the N1 is fast when compared to that of the vehicles approaching from the on-ramps. The rate of bottleneck dissipation of the Okavango Boulevard off-ramp is evident as the heatmap changes colour from red to yellow to green. There is however an upright bottleneck formation on the Brackenfell Boulevard.

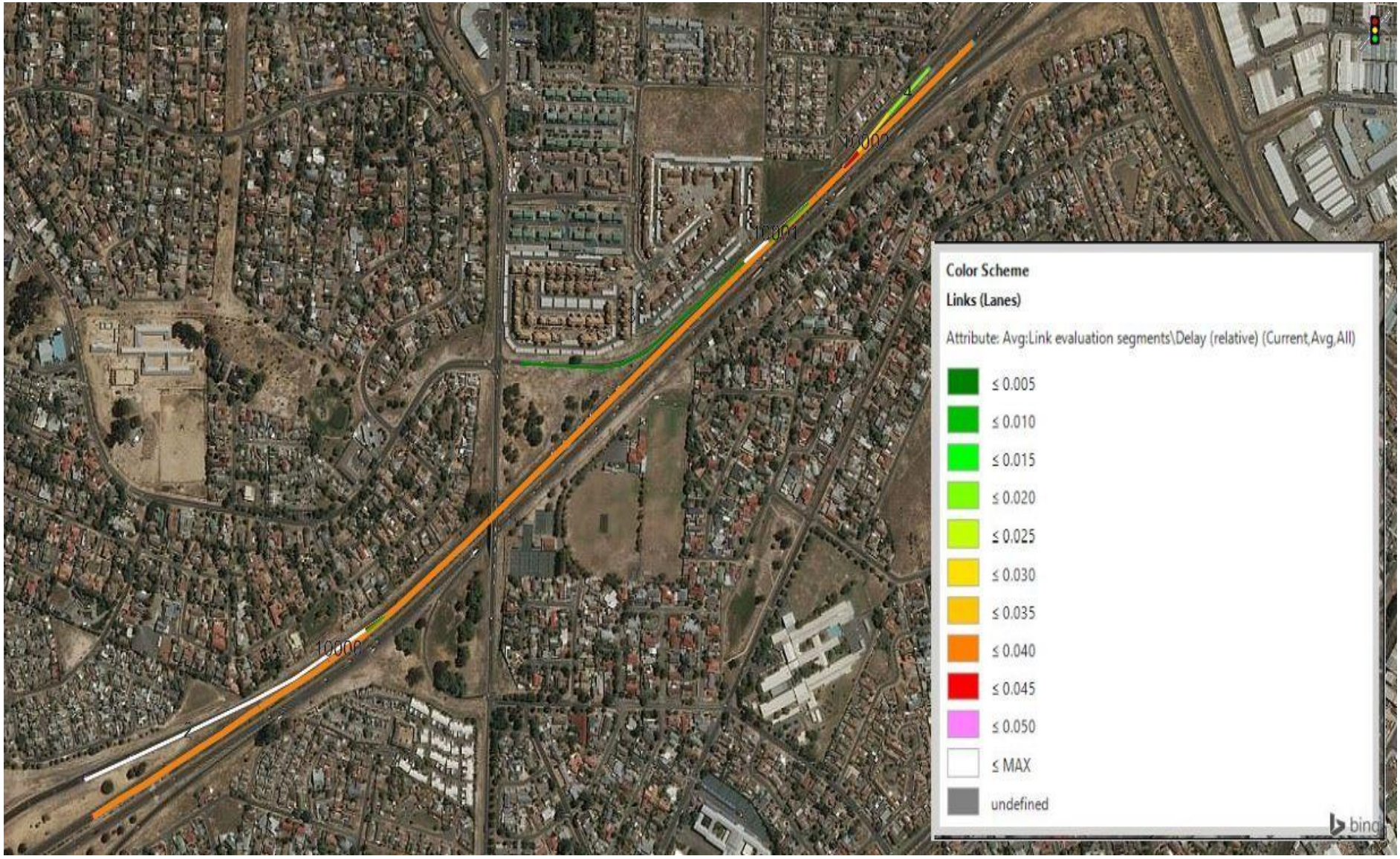

Figure 7-1: Base case scenario delays

7.1.3 Flow relationship and Regression analysis

Flow relationships were analysed along the national road N1 at four different locations. The locations were selected based on the observation that traffic flow characteristics vary significantly at these locations mainly due to the presence of off- and on-ramps and also due to the general road geometry.

- Location 1 Before R300
- Location 2 Between R300 and Brackenfell Boulevard on-ramp
- Location 3 Between Brackenfell Boulevard on-ramp and Okavango Boulevard off-ramp
- Location 5 After Okavango Boulevard

To better understand the traffic behaviour and flow on the road, it became apparent that existing traffic flow models ought to be incorporated into the analysis. This would allow for a clear comparative analysis at different locations for different remedial actions, that will be proposed and investigated in Chapter 8 of this research project. The following flow characteristics models were used to analyse the base case:

- Greenshields Model,
- Underwood Model,
- Greenberg Model,
- Bell-shaped method

The best-fitting model will be adopted and carried forward to analyse the remedial actions at the different locations. First, it is important to summarise the fundamentals governing the different models. Each method seeks to represent the fundamental relationships with emphasis placed on the speed-density relationship. The resulting algorithms and their principles are summarized in Table 7-1. The general algorithm consists of the following variables: V = speed, K = density, Vf = free flow speed, Kj = jam density, k0 = critical density. The unknown parameters are the free flow speed and the jam density.

Regression analysis was applied to the speed-density curve as opposed to the flow-density and the speed-flow curves due to ease of application by using the steady state equation. The curves were fitted to the PTV VISSIM output data using regression analysis. The results of the curve fitting are represented and discussed in Table 7-3.

Table 7-1: Summary of Fundamental Diagrams Principles and Formulae

Model	**Year developed**	**(Source)**	**Principles**	**Resulting Algorithm (Speed density)**	**Transformation**	**Limitations**
Greenshields	1935	(Zhaoyang & Qiang, 2013) (Danquah, 2010)	A liner relationship between speed and density	$k = kj\left(1 - \frac{V}{Vf}\right)$	$V = V_f - \frac{1}{Kj}K$	Linear relationship is seldom present in many cases
Greenberg	1959	(Zhaoyang & Qiang, 2013) (Danquah, 2010)	Incorporates Fluid dynamics principles to relate speed and density	$K = Kje^{\left(-\frac{V}{V0}\right)}$	$V = V_o Ln\, K_j - VLn(K)$	Does not provide realistic estimates during free flow conditions (source)
Underwood	1961	(Zhaoyang & Qiang, 2013) (Danquah, 2010)	Exponential relationship between speed and density	$K = K_0 Ln\left(\frac{Vf}{V}\right)$	$K = K_j Ln(V_f) - K_o LnV$	It sometimes fails to produce appropriate free flow speed

Model	Year developed	(Source)	Principles	Resulting Algorithm (Speed density)	Transformation	Limitations
Drake *et al.* (Bell-Shaped)	1965	(Zhaoyang & Qiang, 2013) (Danquah, 2010)	Established that the speed density curve has a concave shape at low density.	$K = K_0 \sqrt{2 * Ln(\frac{Vf}{V}}$	$K^2 = 2K_j^2 LnV_f - 2\,Kj^2 LnV$	Inappropriate when estimating data under congested conditions

The first test was to check which model best fits the data. The Underwood Model was found to be the best fitting model at all five locations as depicted in Table 7-2 below, indicating that the traffic data on the N1 case study section was best represented by this model. The model was furthermore used for an analysis of the free flow speed and the critical density.

Table 7-2: Regression Analysis R Squared Results

Model	**Fit (R^2)**
Greenshields	0.93
Greenberg	0.76
Underwood	0.98
Bell-Shaped	0.90

Table 7-3: Best fitting Speed Density Regression Curve

Model	Speed density formula/ Regression Curve	Curve
Greenshields	$u = 119\ (1 - \frac{k}{76.90})$	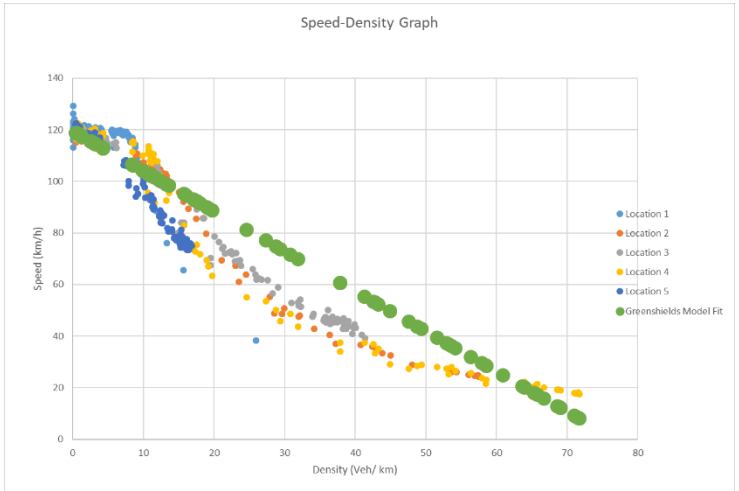

Model	Speed density formula/ Regression Curve	Curve
Underwood	$k = 34\ Ln\ (\frac{130}{V})$	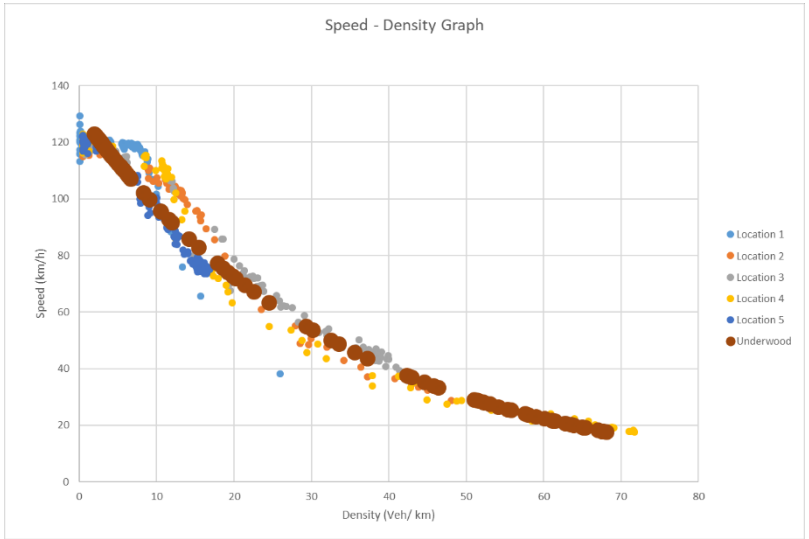
Greenberg	$k = 148 * e^{(\frac{v}{28.3})}$	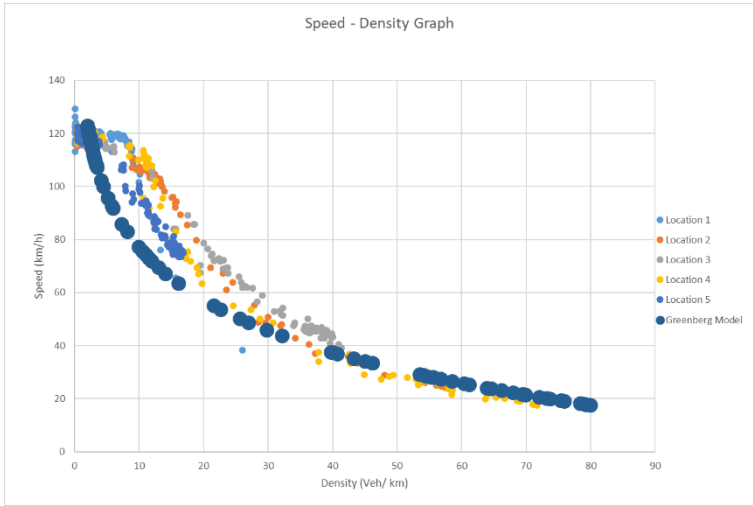

Model	Speed density formula/ Regression Curve	Curve
Bell-shaped	$k = 33.27\ (2 * \ln\left(\frac{110}{V}\right)^{0.5})$	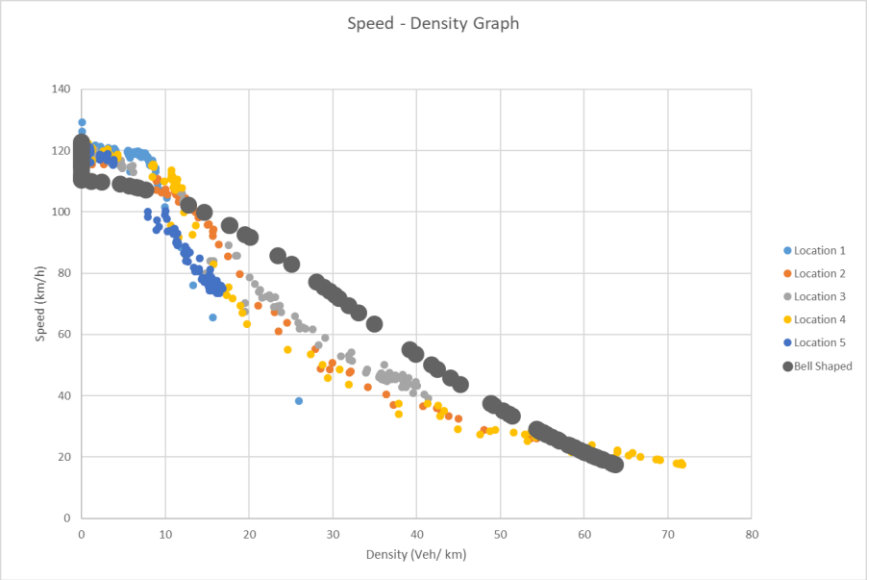

7.2 CCTV observations

7.2.1 Available footage

Video recordings of traffic in the case study area were collected in July 2017. Footage was collected during the morning peak period (05:30 to 08:30) and the afternoon and evening peak period (16:30 to 18:30). The weather on the dates on which videos were recorded was sunny. Visibility was not obstructed. The videos were recorded at three separate locations within the case study. The first video was facing north and provided information on the merge of the R300 with the N1, the second video was facing north and provided recordings of the diversion of traffic from the N1 to the Brackenfell Boulevard on-ramp. The last video was facing south and provided information on the traffic movement from and between the N1 and the Okavango Road off-ramp.

The recordings were used to analyse the traffic conditions in the morning and afternoon peak hours. Video analysis covered the entire week to allow for an understanding of typical variations in behaviour during a week.

7.2.2 Illegal manoeuvres

The observations indicated that vehicles approaching the N1 from the R300 on-ramp often disregarded the solid line markings and merged with the N1 traffic earlier than allowed. This is attributed to the geometry of the merge. The R300 is a two-lane road that merges into a single lane road leading to the merge with the N1. Traffic becomes restricted when the number of lanes drops, creating a backlog. This is exacerbated by the fast-moving vehicles on the N1, that require a careful slow merge. Once the backlog increases and a queue forms, some drivers were observed to ignore the merge on the R300 on-ramp and kept driving as if there were two lanes. These vehicles then cross the solid line to merge with the N1 or move straight into the fast-moving lanes of the N1. This raises the risk of accidents together with instances of unconventional weaving. The unconventional weaving observed in this case is the result of an early merge due to human behaviour. This occurs when vehicles from the right lane move from their lane into the left lane of the N1 at the same point that some vehicles are making an early merge from the R300. This type of early merge from the R300 is dangerous as oncoming traffic from the N1 is fast and not expecting the merge at that location.

Photo 7-1: N1 Video Observations (Bottleneck Formation) looking north

7.2.3 Observed Bottlenecks

Traffic bottleneck formations on the N1 begin at roughly 16:40 and the road becomes heavily congested at roughly 17:10. It was also observed that on a typical day, a traffic bottleneck develops earlier on the R300 merge section before any develops on the N1, resulting in vehicles forming two lanes on a single lane stretch. This is attributed to the prior merge of the R300 from a two-lane road into a single lane. There is a pronounced number of lane changes from the inner to the outer lane on the N1 as traffic moves faster on the outer lane. It is also because the inner lane slows down due to the merging traffic. The pronounced lane changed raises the risk of accident on this section of the road. It was observed that lane changes are often abrupt from slow moving on the R300 or the heavily congested slow and outer lane to the fast lane. The risk of an accident is high in this case due to the speed differential of the vehicle changing lanes and the vehicle approaching from the N1 on the fast lane. Traffic on the R300 is merging at a curve where visibility is limited. This is a factor for the quick queue formation as drivers try to ensure that they

can see the oncoming through vehicle and that the through vehicles can also see them. The location of the merge at a curve appears to raise the risk of accidents.

Past the R300 merge point, slow moving vehicles begin to gain speed. However, this is interrupted at the succeeding on-ramp from the Brackenfell Boulevard which is located 500 m upstream of the Okavango Boulevard off-ramp. The effect of this on-ramp is not as pronounced as that of the R300 on-ramp because fewer vehicles are merging with the N1.

500 m downstream of the Brackenfell Boulevard on-ramp is the Okavango Rd off-ramp from the N1. Unconventional weaving was observed to occur at the 500 m stretch between the Brackenfell Boulevard on-ramp and Okavango Boulevard off-ramp. The weaving manoeuvre at this location is termed unconventional because there is no auxiliary lane precipitating the manoeuvres and so it is not a typical Type A weave. Weaving on this section is a result of the early merging to Okavango Boulevard from the N1 which weaves with vehicles exiting the Brackenfell Boulevard on-ramp. As most traffic from Brackenfell Boulevard on-ramp moves to the N1 and sufficient traffic from the N1 moves to the Okavango Boulevard, this type of weaving is most pronounced and occurs often on this stretch of the road. It was noted that most cars from the Brackenfell Boulevard on-ramp were changing lanes to the N1 when compared with the number of cars proceeding from Brackenfell Boulevard on-ramp to Okavango Boulevard.

Photo 7-2: N1 Video Formation Brackenfell Boulevard on-ramp -Okavango Boulevard looking south

The video recordings did not capture any accidents due to weaving or early merging during the period of the recordings. However, there were numerous near-miss incidents where the risk of such accidents occurring was heightened. Nine such incidents were recorded on the R300 on-ramp, and five on the Brackenfell Boulevard on-ramp.

7.3 VDS Data analysis

Traffic fundamental relations were analysed to assess the operations of the traffic on the N1. Volume speed diagrams for the case study (N1) were assessed along the studied stretch of the N1. Scatterplots of average speed versus average flow are illustrated in Figure 7-2. Aggregated 1-hour observation data from the study site was used to construct the scatter plot.

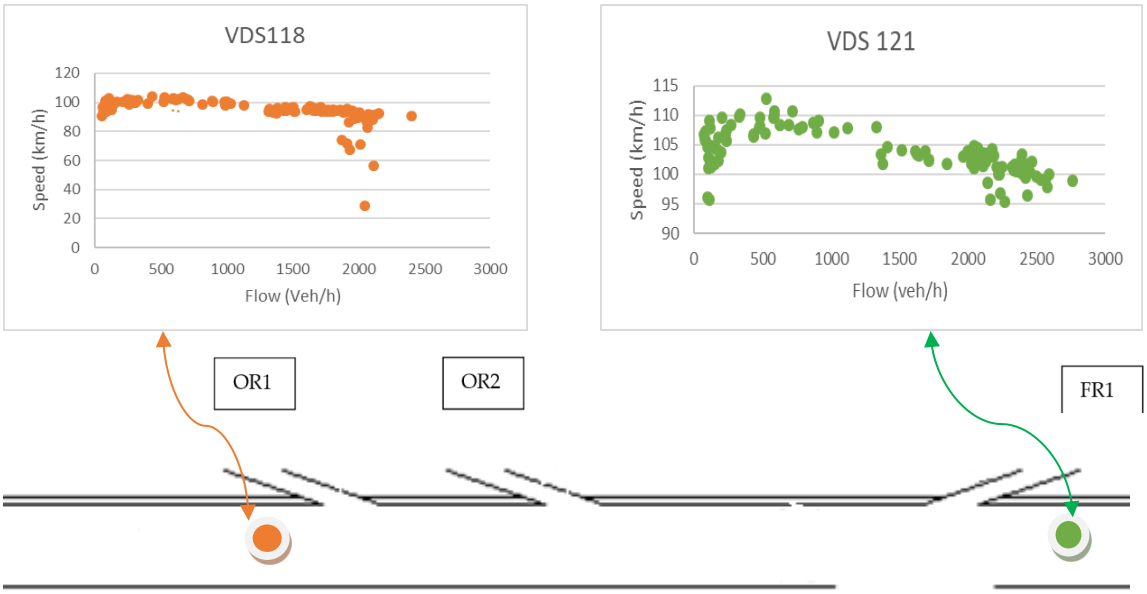

Figure 7-2: Fundamental graphs produced from collected data

The fundamental graphs above depict a carriageway with a constant number of lanes along its stretch. The first section has a VDS118 before the on-ramp OR1 (R300), which is a two-lane undivided section. This section is upstream of the bottleneck and will reach the bottleneck at speeds below 100 km/h and flows above 2000 veh/h. The second section is far downstream and susceptible to upstream effects, such a congestion. The downstream congestion is due to the two successive on-ramps and traffic entering the stream from the ramps.

It can be seen that the stream from on-ramp 1 (OR1) does not receive enough range to dissipate before being joined by on-ramp 2 (OR2) at a speed of between 60km/h and 20 km/h. The fundamental graph is horizontal to slightly parabolic which indicates that the road is operating in free flow until such time as an optimum flow is reached. After this point an increase in congestion results with a decrease in both speed and flow.

The stretch of road passing between Brackenfell Boulevard on-ramp and Okavango Boulevard is a two-lane undivided carriageway. The traffic speed further reduces in anticipation of the on-ramp downstream. The reduction in speed is attributed to weaving manoeuvre of vehicles from the extreme lanes navigating the road to each off-ramp or to reach the fast lane. The fundamental graph takes on a parabolic shape. The parabolic shape indicates that free flow only occurs when the density is zero.

VDS 121 is downstream of the off-ramp (FR1). The speed flow diagram depicts erratic driving behaviour as vehicles manoeuvre to off-ramp. The lower end of the diagram is attributed to the downstream off-ramp and on-ramp. Due to the short succession of the ramps, vehicles tend to weave resulting in reduced speed, safety and capacity. Upstream of the section, capacity is significantly reduced. It must be noted that a major off-ramp is located upstream of the section.

7.4 Accidents Statistics

Photo 7-3: Incidents and Accidents occurrence on the N1 Case Study area

Photo 7-4: Accidents occurrence on the N1 Case Study area

Accident and incident data were provided by SANRAL and covers dates from January 1 to April 30 in 2017. The data comprised of the date and time of the accident, the type of accident or incident, severity, cause, and location in terms of coordinates. No accident footage was available for review, which could assist in pinpointing the actual cause of accidents. Accident analysis was based on imposition of accident data on aerial maps. This made it difficult to ascertain accidents caused by erratic lane changes and weaving manoeuvres with certainty.

The incident rate on the road over the four months period was found to be 10 incidents per km while the accident rate was approximately 2 accidents per km over the four months. "Incidents" refers to obstructions such as a broken-down vehicle, lost loads, protests etc.

Review of most of the accidents recorded (in the SANRAL data) indicates that there is a high concentration of multiple vehicular accidents at the identified case study segment. Multi-vehicular accidents can be attributed to numerous things such as sideswipe, head-on collision, and bumper bash. This type of accident is common in the afternoon and evening when visibility is compromised. They are also common in areas were weaving occurs (Golob, et al., 2004).

Single vehicle accidents are evident in the morning and during the rest of the day. All in all, the majority of accidents on the section under consideration are multiple vehicles accidents occurring in the evening. Accidents are more pronounced during peak hour. It was observed that directional accidents occur when the peak stream of traffic is in that direction.

During the afternoon and evening peak periods, when travelling speeds are lower, accidents with minor injuries and damages (like bumper bashes and sideswipes) are more likely to occur. From the available photographs of the aftermath of serious accidents, no specific pattern is evident. The final locations of where vehicles involved in accidents end-up are either on the left-hand side or to the right-hand side of the outbound carriageway.

The presence of multiple accidents on the section of the N1 under consideration are attributed to the geometry of the road. Three of the recorded accidents occurred either downstream of the merge or at the merge of the R300 with the N1. This is thought to be the result of the presence of a curve along the N1 which sees the R300 and the N1 merge being located at a curvature with limited sight distance. It must be noted that the R300 also approaches the merge at a curvature increasing the chances of accidents to both streams of traffic. Three of the accidents also occurred at the area where weaving is prominent, between the R300 on-ramp and the Okavango Boulevard.

8 IDENTIFICATION OF REMEDIAL ACTIONS

8.1 Introduction

The validated base case model analysis discussed in Chapter 7 indicates that there are numerous deficiencies in the flow of traffic on the N1 case study. The model indicates bottlenecks between the R300 on-ramp up to the Okavango Boulevard off-ramp. In a high volume of traffic, lane changes and weaving occur especially between the Brackenfell Boulevard on-ramp and Okavango Boulevard. Other identified problems emanate from the geometric (horizontal alignment, with respect to the R300 on-ramp merging the freeway at a curvature) design of the road and human behaviour. To counter the effects of the geometry and with the aim of resolving the congestion and bottlenecks, remedial actions are proposed. The proposed remedial actions are bulleted below.

- Action 1: Ramp metering on the Brackenfell Boulevard on-ramp
- Action 2: Auxiliary lane between the Brackenfell Boulevard and the Okavango Boulevard
- Action 3: Increasing the R300 on-ramp capacity
- Action 4: Combined effect of increase R300 on-ramp capacity and ramp metering on the Brackenfell Boulevard on-ramp

These remedial actions were modelled using PTV VISSIM based on the calibrated base case study. The remedial actions are analysed and discussed in subsequent sections. Traffic flow response was then analysed for the following four locations along the N1:

- Location 1 Before R300,
- Location 2 Between R300 and Brackenfell Boulevard on-ramp,
- Location 3 Between Brackenfell Boulevard on-ramp and Okavango Road
- Location 5 After Okavango Boulevard.

The analysis will be based on the proposed remedial action and its effect at the different locations along the N1. Concentration in the discussion of the remedial action is centred around location 3 which is the area that experiences the most weaving action. Annexures B and C provide fundamental diagrams that could be used for reference purposes for other locations.

8.2 Ramp metering

Ramp metering is a freeway management tool where traffic signals are installed on freeway on-ramps to control the frequency that vehicles enter the freeway. It reduces freeway congestion by limiting and controlling the amount of traffic entering the freeways. It is a system of ensuring effective freeway management while also addressing safety issues and congestion. Ramp metering is proposed in this study to be installed on the Brackenfell Boulevard on-ramp to limit the number of vehicles entering the N1 thereby preventing a drop in capacity on the freeway and, concurrently, congestion on the ramp.

A ramp-metering scenario was tested in PTV VISSIM by first defining the position of a ramp meter and signal head along the Brackenfell Boulevard on-ramp and assigning it properties that would enable vehicles to enter the N1 with minimum interruption to the free flowing freeway vehicles while also ensuring that the Brackenfell Boulevard on-ramp and adjoining streets do not become congested. Brackenfell Boulevard on-ramp was modelled as a single lane on-ramp that transits into an acceleration lane. The general fixed-time ramp-metering logic was used that resulted in the ramp-meter signal turning green when a vehicle approached the signal head. This signal remained green until it the vehicle reached the departure detector as shown in Figure 8-1. Once the departure detector was reached, the signal then turned red and remained so until there was either a new vehicle detected in the approach detector, the vehicle on the departure detector had moved or the meter signal had been red for a predefined fixed time in seconds. For purposes of modelling, the fixed time was changed from the default 3 seconds to 4 seconds to achieve the desired ramp capacity. The desired capacity was assessed by visually observing interactions as the model ran.

Figures 8-1 and 8-2 provide an indication of the ramp-metering scenario that was ran in PTV VISSIM and the delay heatmap of the section when ramp metering was adopted. The green portion on Figure 8-1 indicates the ramp-meter signal that turned red or green depending whether there was a vehicle in the approach detector (in white) or the departure detector (in blue).

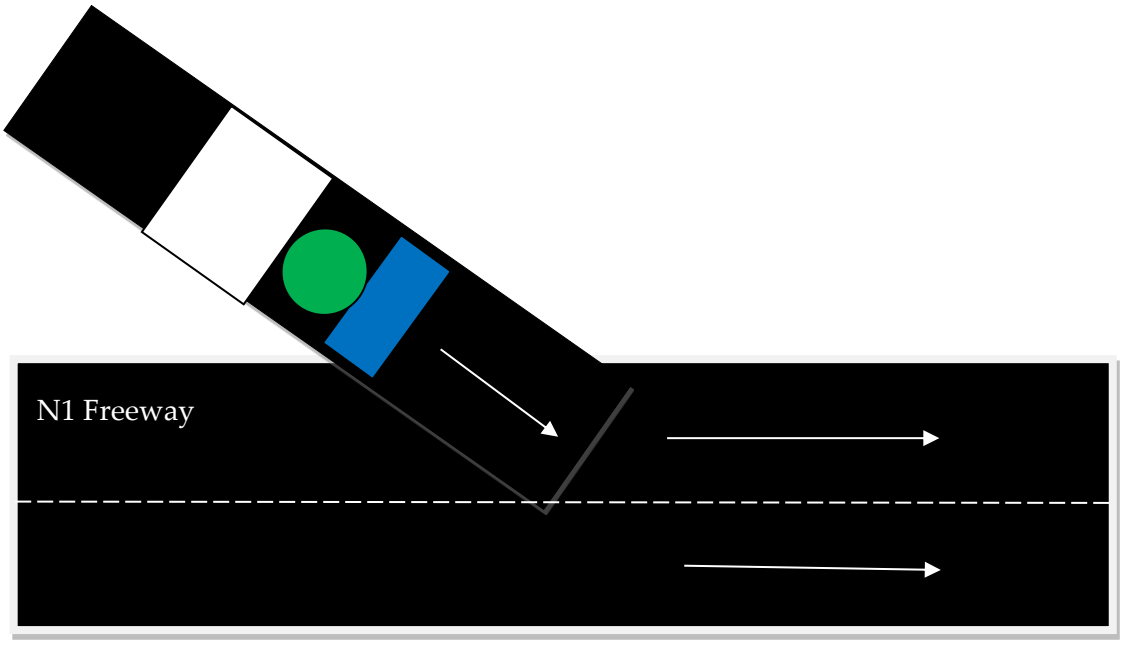

Figure 8-1: Ramp-Metering Layout

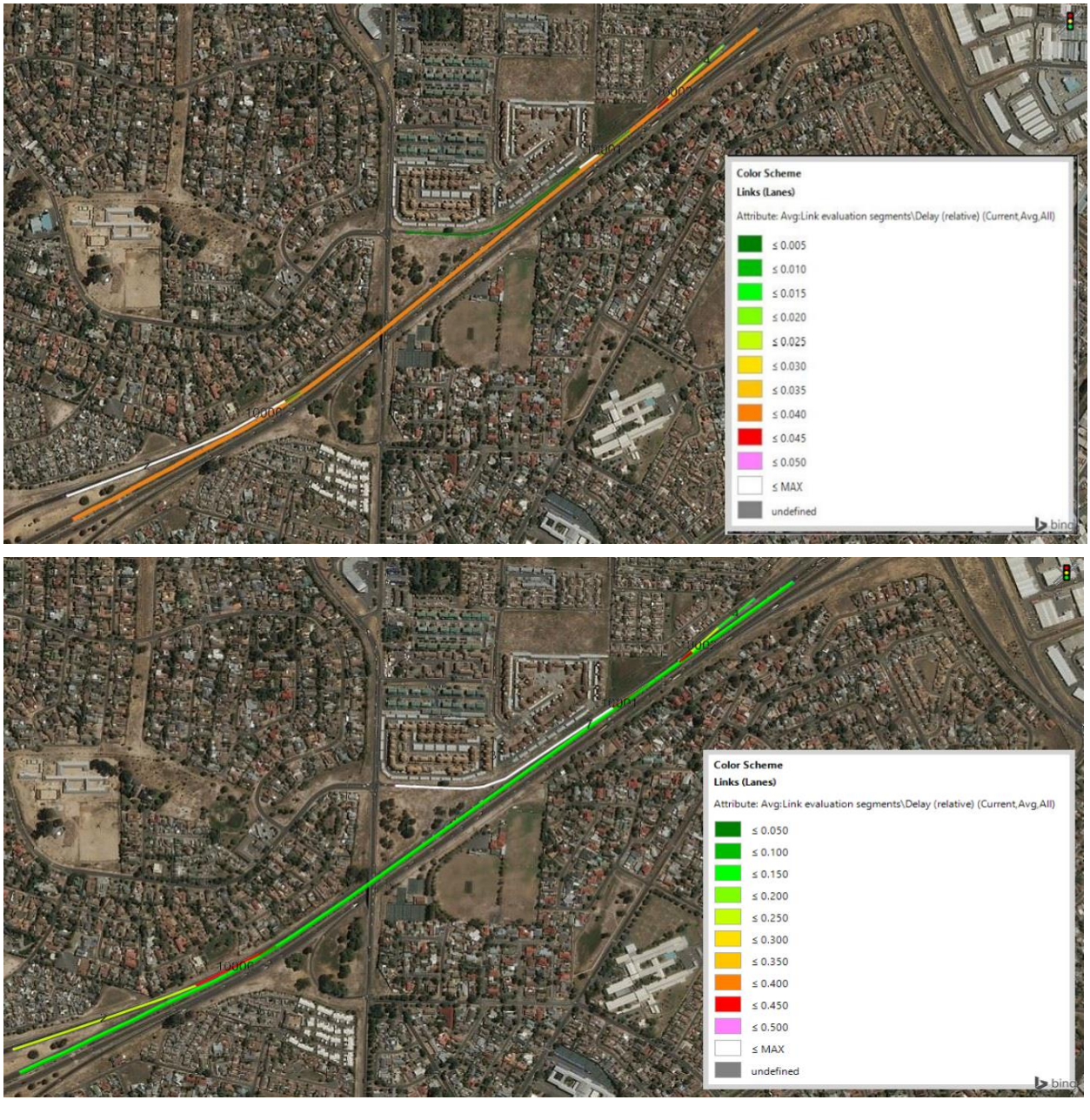

Figure 8-2: Comparative representation of delays, base case (top) vs ramp metering (bottom)

The comparison analysis of the base case scenario and the delay heat map as shown in Figure 8-2 indicates that there is an improvement on the delay length on the N1 and the R300. There is however an increase in delays on the Brackenfell Boulevard on-ramp that is attributed to the slow dissipation of queues due to the ramp meter. Okavango

Boulevard experiences similar delays when ramp metering is employed at Brackenfell Boulevard compared to the base case scenario.

The results from the ramp-metering intervention analysis and the regression analysis indicate that the free flow speed on the freeway between the Brackenfell Boulevard on-ramp and Okavango Boulevard has reduced from the base case free flow of 128.9 km/h to 123.47 km/h. The critical density for the ramp metering stands at 39.87 veh/km when compared to the base case critical density of 36.01 veh/km. Ramp metering therefore results in more vehicles per kilometer and a generally increased volume and capacity. The results indicate that the implementation of a ramp meter at the Brackenfell Boulevard on-ramp will increase the capacity of the N1 particularly between Brackenfell Boulevard on-ramp and Okavango Boulevard.

The ramp meter was applied to the Brackenfell Boulevard on-ramp and not the R300 after identifying the area of high weaving to lie between Brackenfell Boulevard on-ramp and Okavango. In this case it was assumed that traffic from R300 would have minimal effect on the weaving and that traffic from Brackenfell Boulevard on-ramp going to the N1 is the main cause of the weaving. The configuration of the ramp geometry brought constraints relating to the capacity of vehicles that it could carry. The capacity of the ramp could only be increased by increasing the length of the Brackenfell Boulevard on-ramp which was not possible in this case due to the existing geometry. The ramp capacity was exceptionally low to allow for a ramp metering which only became obvious during model running and analysis. The other factor contributing to the results is the type of metering that was deployed on the ramp. The results on the Brackenfell Boulevard on-ramp indicate that the fixed time controller was not suitable for this ramp and that the selected four seconds were unsuitable for the overall road section configuration because it is not flexible, i.e. does not change with changing demands. Rather, a traffic responsive controller should be considered that is influenced by the freeway traffic together with the ramp traffic volumes and that looks as both upstream and downstream freeway volumes and automatically adjusts accordingly. This may substantially increase the capacity of the Brackenfell Boulevard on-ramp.

8.3 Auxiliary lane between the Brackenfell Boulevard and the Okavango Boulevard

An auxiliary lane is the portion of a roadway between interchanges, or an on-ramp and off-ramp that adjoins the travelled way. It is usually used to allow drivers room to increase or decrease their speed when entering or exiting the travelled way. It is envisioned that an addition of an auxiliary lane can be used for weaving, as a climbing lane for trucks and to maintain a uniform level of service on the N1 freeway. For purposes of analysing the effect of an auxiliary lane on the case study, an auxiliary lane was added

between the Brackenfell Boulevard on-ramp and Okavango Boulevard off-ramp. The included auxiliary lane width was taken to be equal to the freeway through lane. A representation of the auxiliary lane input is depicted in Figure 8-3 below.

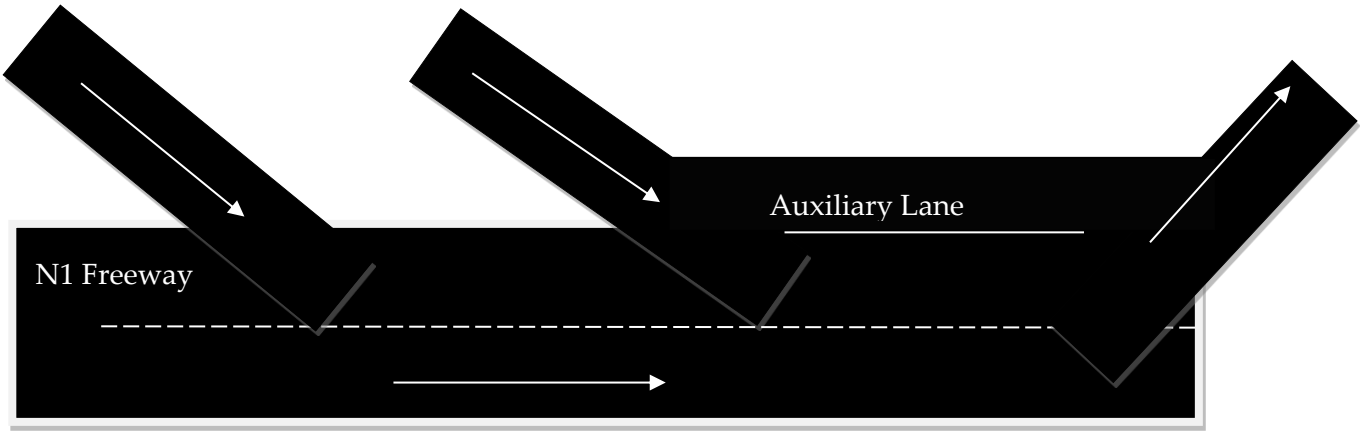

Figure 8-3: Auxiliary Lane Layout

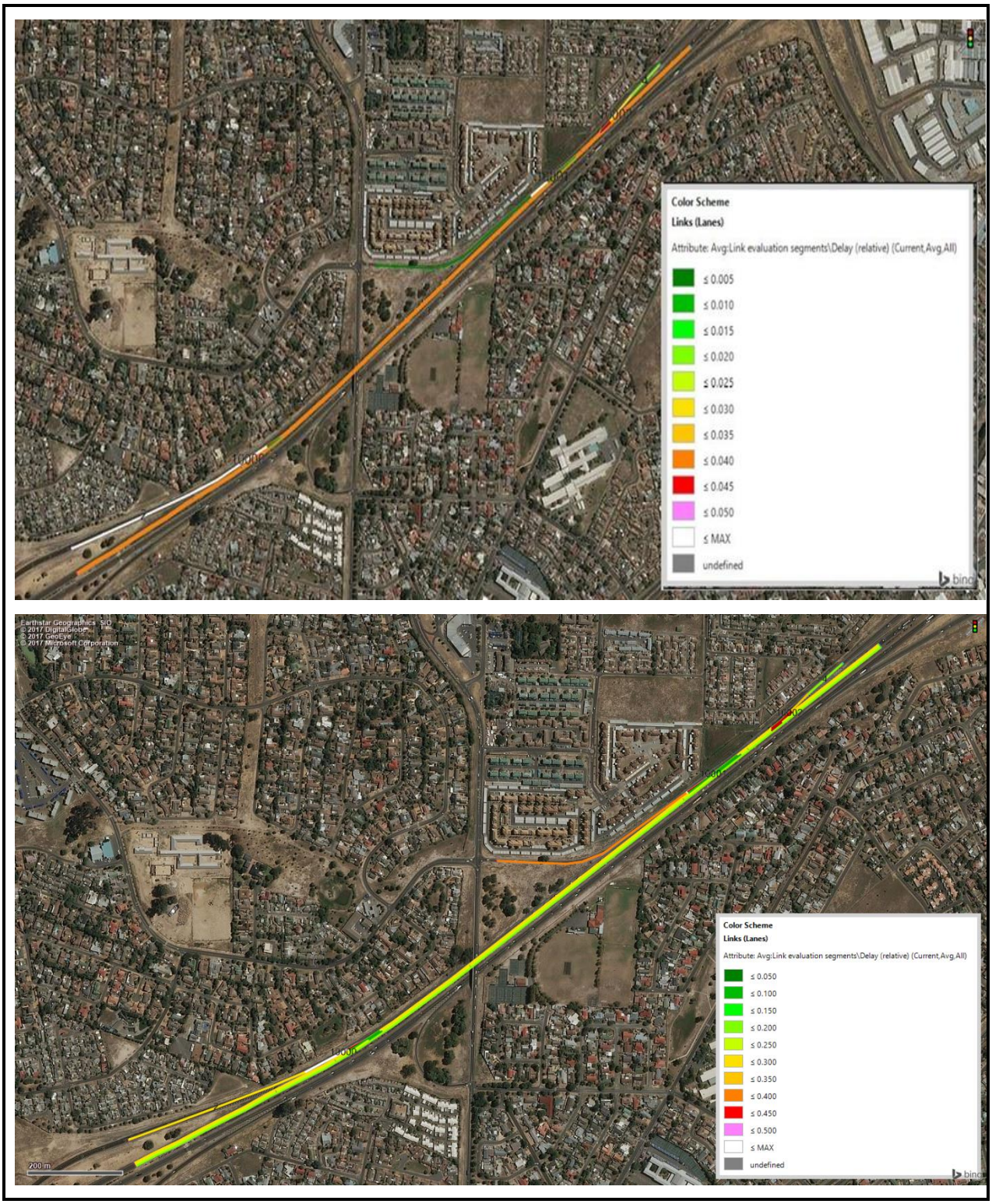

Figure 8-4: Comparative representation of delays, base case (top) vs an auxiliary lane (bottom)

From the analysis and in reference to the fundamental flow diagram the following can be deduced:

- The overall results from including an auxiliary lane show that the free flow speed on the freeway has reduced from the base case free flow of 128.9 km/h to 121.35 km/h.
- The critical density when an auxiliary lane is included stands at 32.1 veh/km when compared to the base case critical density of 36.01 veh/km.

The delay heatmap shows a situation whereby there is a reduction in delay on the R300 on-ramp, on the area between the Brackenfell Boulevard on-ramp and the Okavango Boulevard and on the N1.

The results indicate that the construction of an auxiliary lane between the Brackenfell Boulevard on-ramp and Okavango Boulevard will increase the capacity of the N1 particularly between Brackenfell Boulevard on-ramp and Okavango Boulevard. This is attributed to an increased movement between the freeway and the auxiliary lane. Some traffic on the Brackenfell Boulevard on-ramp will continue on the auxiliary lane towards Okavango Boulevard. There is a noticeable increase in the number of vehicles changing lanes between the Brackenfell Boulevard on-ramp and Okavango Boulevard when an auxiliary lane is introduced. Vehicles from Brackenfell Boulevard on-ramp travelling onto the N1 remain on the auxiliary lane longer and only make lane changes towards the end of the auxiliary lane, hence increasing weaving manoeuvres. Vehicles travelling from the N1 onto Okavango Boulevard will make lane changes from the start of the auxiliary lane, on the middle portion of the auxiliary lane or at the end of the auxiliary lane. This increases the lanes and lengths at which weaving occurs hence reducing the average free flow speed on the section.

A graphical comparative analysis of the difference between the base case and the auxiliary lane in Figure 8-6 shows that the two speed-density curves' slope vary by 0.05 which is deemed insignificant for purpose of analysis. The auxiliary lane curve is however shifted downwards indicating an overall reduction in the average speed. The analysis of the densities indicate that vehicles tend to congest quickly in the base case when compared to the auxiliary lane.

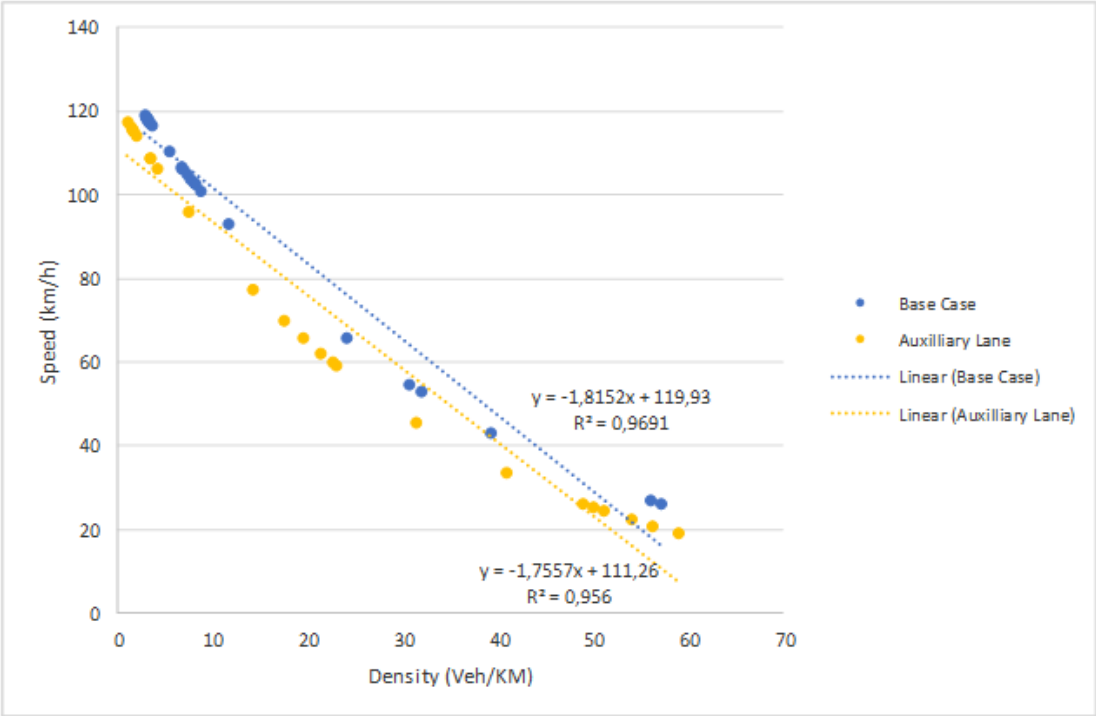

Figure 8-5: Auxiliary Lane Speed Density Graph Compared to the Base Case

8.4 Increasing R300 capacity

The third tested scenario was to increase the capacity of the R300 by means of constructing a second lane making the ramp a two-lane on-ramp. In order to achieve lane balancing, an auxiliary lane was also included from the R300 on-ramp to the Okavango Boulevard. The schematic of the R300 ramp with increased capacity and lane balancing is shown in Figure 8-6. In Figure 8-8, the comparative representation of delays between the base case and increasing the R300 capacity is shown.

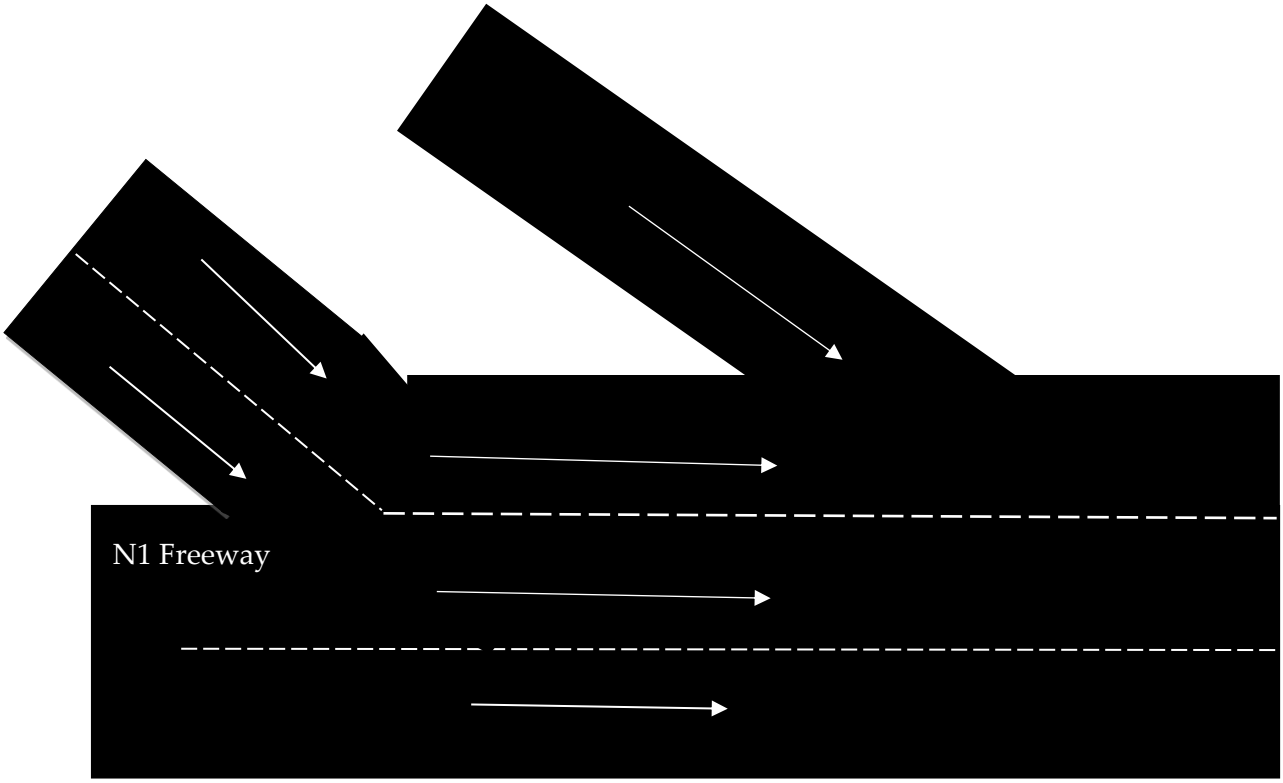

Figure 8-6: Increasing the R300 Capacity Layout

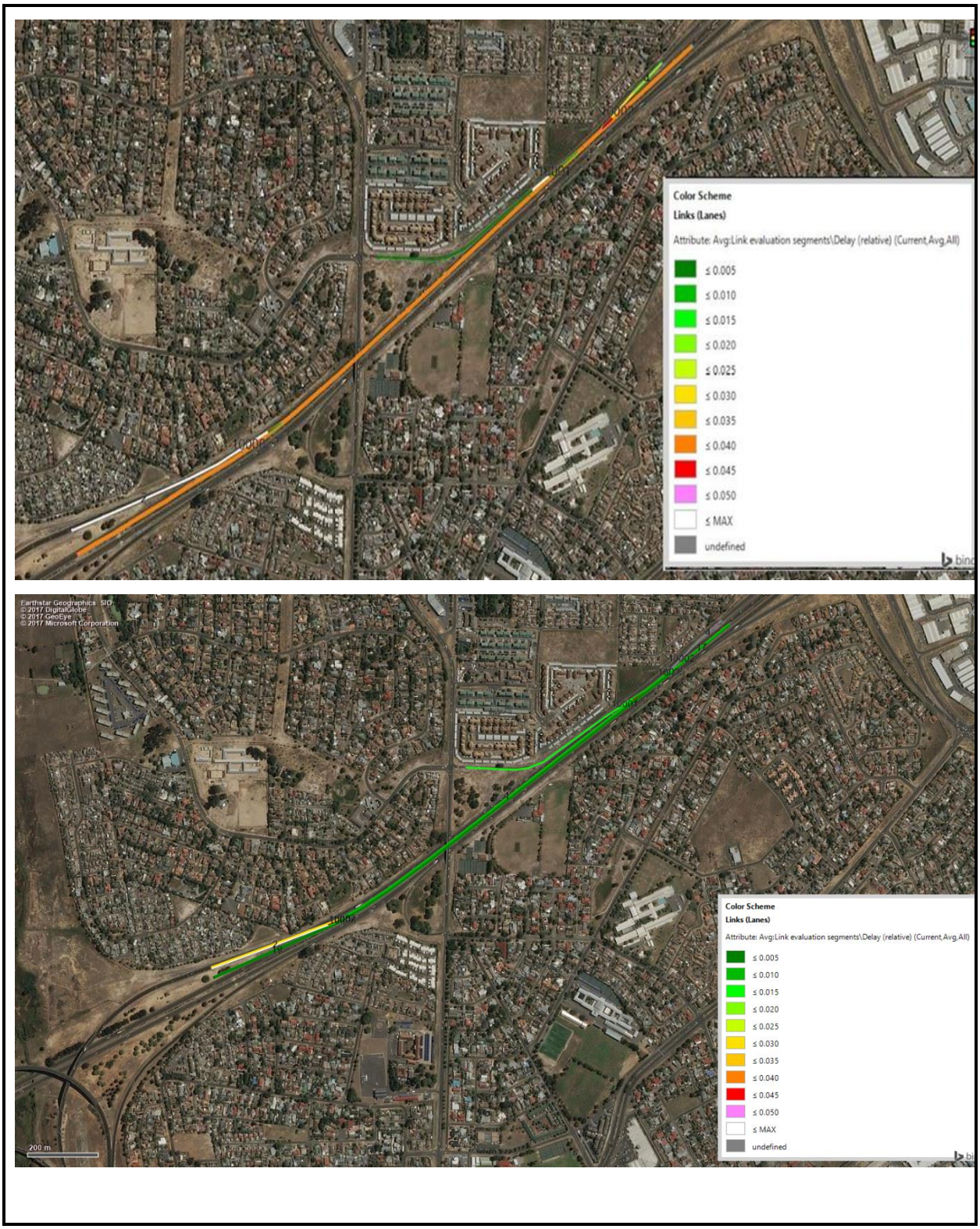

Figure 8-7: Comparative representation of delays, base case (top) vs increasing the R300 capacity (bottom)

There is a noticeable difference in the delays experienced on the road section when the R300 capacity is increased. There is a lowering of delays on the N1, the Okavango Boulevard and the Brackenfell Boulevard. Delays on the inner lane of the R300 on-ramp remain high whilst the delays on the outer lane have reduced significantly. The high delays on the inner lane are a result of the queue backup due to cars not accepting gaps frequently due partly to the high speeds on the N1.

The results of the regression analysis like the two other scenarios already discussed, shows that increasing the R300 capacity would result in capacities higher than those of the base case. However, the results from the regression analysis indicate that by increasing the ramp capacity the free flow speed surpasses that of the base case scenario at 134.4 km/hr with critical density of 35.2 veh/km.

Provided that we are analysing the free flow speed and critical densities of vehicles under free flow, it is imperative to understand the interface between the ramp and the freeway and its functioning during free flow constraints. In essence, under free flow conditions, traffic is uniform with low speed fluctuations and no congestion. The ramp traffic flow will also be uniform without congestion or backup on the ramp although the speed will be lower than that of the freeway. Merging of the freeway and ramp traffic will be smooth as there are enough gaps in the freeway traffic to accept ramp traffic. This operation will continue smoothly except when the downstream backup begins, demand increases, or accidents happen.

With an increased R300 capacity, there would not be many vehicles backed up on the R300 on-ramp. Instead, vehicles would be able to accept gaps at much safer higher speeds and rates. This assumes that the downstream traffic would be the same as that of the base case. Vehicles entering the freeway will have a chance to accelerate first before entering the freeway and would do so at much higher speeds with lower speed differential between the entering vehicle and the freeway traffic stream. The lower speed differential means that vehicles can maintain a higher free flow speed when compared to the base case.

When looking at the rate of lane changes per second, there is a little difference in how traffic behaves in cases of increasing the R300 capacity when compared to the base case. In fact, the rate of lane change and consequently weaving, increases very slightly when the R300 capacity in increased. This is because there would be more gaps to manoeuvre and less or no vehicle backup downstream of the freeway and on the R300 on-ramp. The results also indicate that the number of weaves is not hugely affected by the volume on the on-ramp but more so by the capacity of the freeway.

8.5 R300 capacity increase and RAMP metering.

The last tested scenario was to check the combined effects of increasing the R300 capacity with lane balancing together with incorporating the RAMP meter at the Brackenfell Boulevard on-ramp. The schematic representation of the layout of this scenario is provided in Figure 8-9. In Figure 8-10, the comparative representation of delays between the base case and increasing the R300 capacity together with ramp metering is shown.

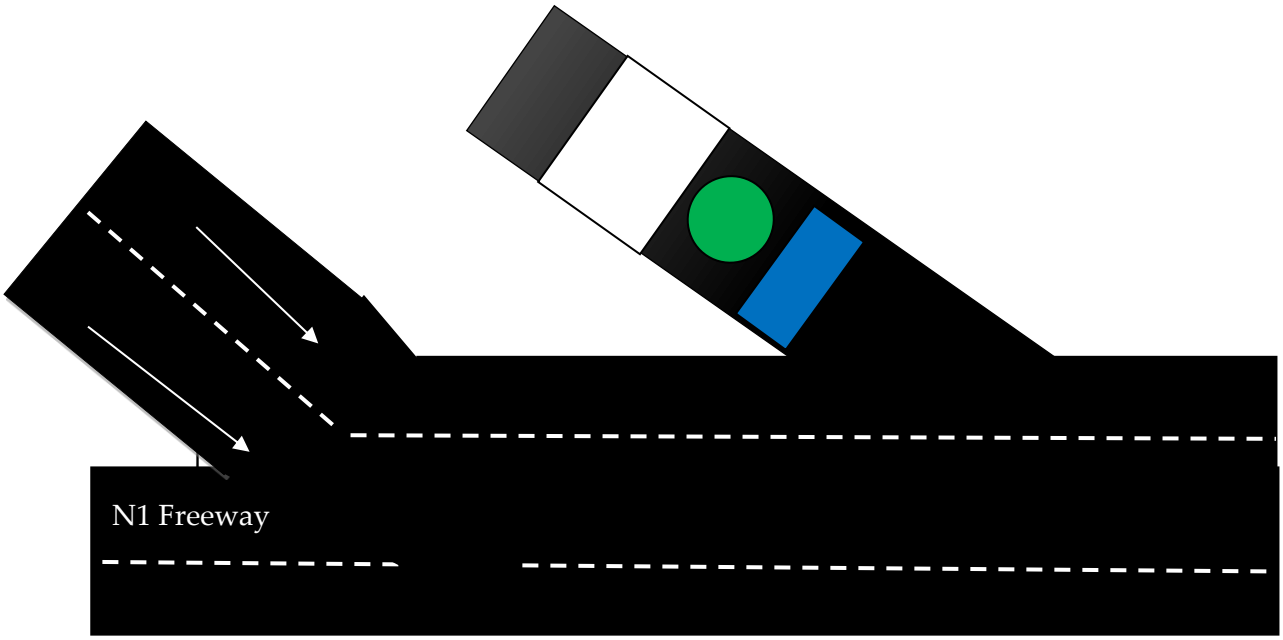

Figure 8-8: Increasing the R300 Capacity and Applying Ramp Metering on Brackenfell Boulevard on-ramp Layout

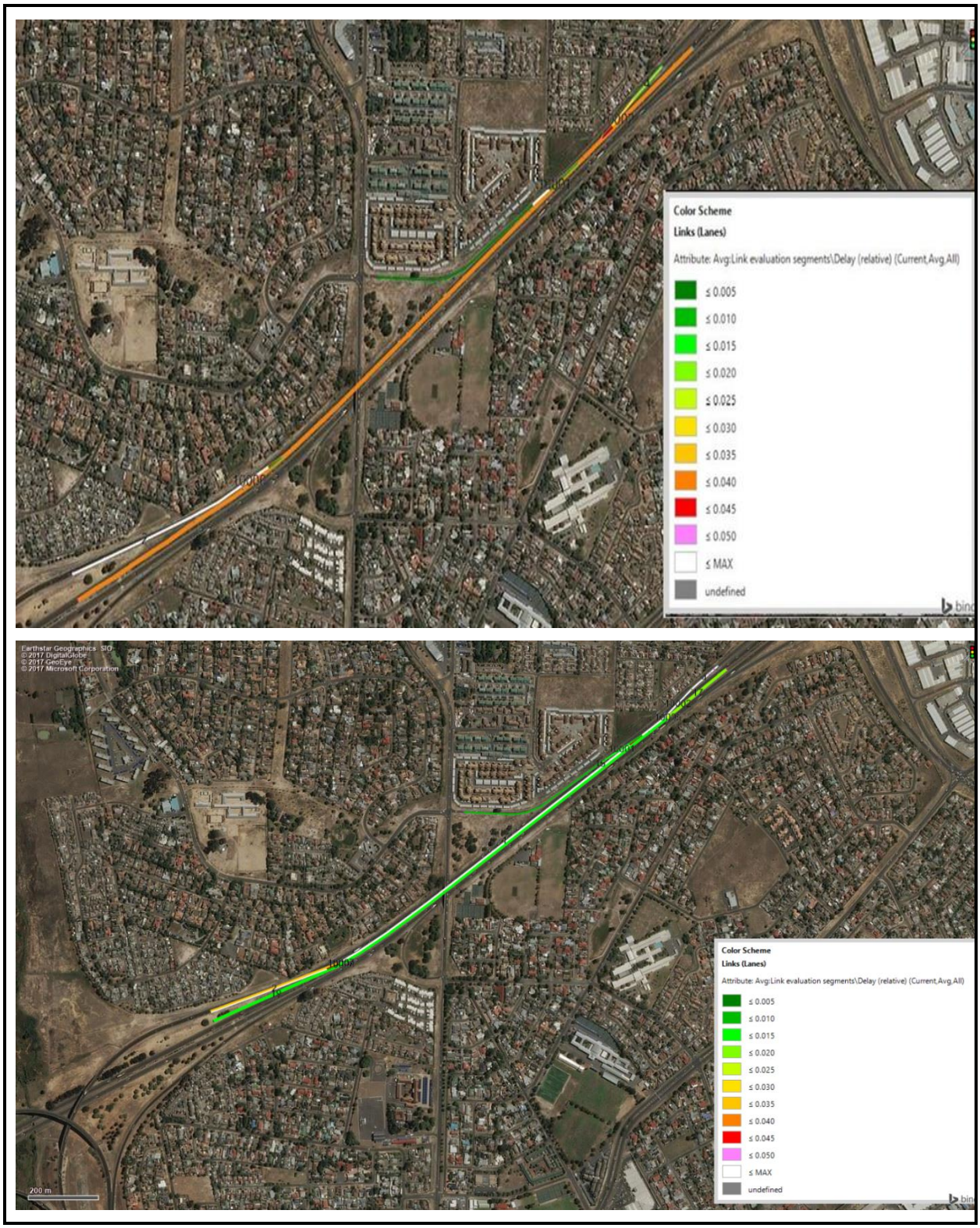

Figure 8-9: Comparative representation of delays, base case (top) Vs increasing the R300 capacity and implementing ramp metering (bottom)

There is an improvement in the delays on the outer lane of the N1, and the left lane of the R300 on-ramp. The level of delays on the Brackenfell Boulevard remains the same. However, there is an increase of delay to the right lane of the R300 on-ramp. The increased delays on the right lane of the R300 result from the queue formation of vehicles trying to find a suitable gap to enter the highway. The delays on the auxiliary lane are the highest indicating that traffic with the destination of the Okavango Boulevard keeps mostly to the auxiliary lane. The other reason for the increased delays is because of traffic from the Brackenfell Boulevard which enters the stream of traffic on the N1 upstream thereby increasing the delays of vehicles downstream. The improved (reduced) delays on the Brackenfell Boulevard are a result if the auxiliary lane that spans from the R300 on-ramp and continues past the Brackenfell on-ramp.

The combined effect of ramp capacity increase and the ramp metering provides a free flow speed of 122 km/h and critical density of 187.5 veh/km which is higher than that of the base case. The results indicate that the ramp meter has a higher effect on controlling and lowering the free flow speeds than the increased ramp capacity. The effect of the increased capacity will be nullified by the ramp meter. Under free flow conditions, vehicles will travel faster downstream of Brackenfell Boulevard on-ramp , however upon reaching Brackenfell Boulevard on-ramp congestion would have formed as a result of a backed-up vehicles on the Brackenfell Boulevard on-ramp and the smaller gaps available for acceptance. Vehicles' speed will reduce further while maintaining higher headways than the base case.

When looking at the rate of lane changes per second, vehicles behave in the exact same manner as when the R300 capacity is increased. This stresses further that the rate of weaving is proportional to the volume on the freeway and not necessarily the capacity and characteristic of the on-ramp.

8.6 Result summary and limitations

The remedial actions discussed above have all shown different levels of improvements to the delays when compared to the base case. Increasing the R300 capacity has shown to have the highest impact in terms of improved delays. It results with free flow speeds higher than those of the base case and critical density slightly lower than the base case as seen in Table 8-1 below. The lowered densities and higher flow rates support the results of the delay heat maps and indicate an increased balanced flow where drivers are maintaining high speeds even at minimal densities.

Table 8-1: Summary of the Speed Density Results from Regression Analysis for Proposed Remedial Actions

Remedial Action	**Critical density Ko**	**Free flow speed Vf**	**Notable change to design (road geometry)**
Base Case (As modelled)	36,7	128,9	None. Base case scenario.
Ramp Metering (Brackenfell Boulevard on-ramp)	39,8	123,2	None. Geometry remains the same
Auxiliary Lane	32	121,3	An additional lane at the point of measurement
Ramp Capacity Increase (R300 on-ramp)	35,2	134,4	An additional lane at the point of measurement
Capacity Increase and Ramp Metering	35.8	122,4	An additional lane at the point of measurement

The worst-case scenario was found to be the implementation of ramp meter on the Brackenfell Boulevard. Based on the Table 8-1 the ramp metering shows increased densities and lower speeds at the point of data collection. This demonstrates that although there is an improvement on flow and capacity within the network, there is congestion at the point of data collection between the Brackenfell Boulevard on-ramp and the Okavango Boulevard off-ramp.

9 CONCLUSION

The objective of this study was to assess the characteristics of unconventional weaving traffic within freeway sections that result from operational constraints, thereby gaining a more detailed understanding of unconventional weaving behaviour, causes and possible solutions. Unconventional weaving traffic was defined as that weaving that is not conventional to the definition in the HCM (2010).It refers to excessive lane changing or weaving that occurs as a result of the geometry of the road, illegal behaviours, disregard of traffic marking etc. For purposes of this study the South African National Road N1 in the Western Cape between the R300 on-ramp and the Okavango Boulevard was selected as the case study. The section of the road under consideration experiences unconventional weaving manoeuvres resulting from the short distance between successive on-ramps (R300, Okavango Boulevard), disregard of the lane markings (at the R300 on ramp) and geometry of the section of road (no auxiliary lanes).

To understand the flow characteristics of the selected road segment, raw data that was provided by SANRAL was used for analysis and to produce preliminary traffic flow information and graphs for the base case. Microscopic analysis using PTV VISSIM was done to further get an understanding of flow behaviour in and around the section of the road under consideration. The assessment of the video recording, PTV VISSIM model on the base case and the raw data both for traffic and accidents indicated that there were a few problems on site contributing to weaving and decreased road safety. The base case model indicated that weaving occurs most between Brackenfell Boulevard on-ramp and Okavango Boulevard off-ramp. It was also determined that weaving is highest in heavy traffic. It was difficult to model illegal weaving and effect of lane marking on weaving. However, proof of disregard to lane markings and illegal weaving was seen on the video footage.

Four remedial actions that were hypothesized to reduce the weaving and increase safety on the road were studied. These included (i) the construction of an auxiliary lane on the section between Brackenfell Boulevard on-ramp and Okavango Boulevard off-ramp, (ii) implementation of ramp metering on the Brackenfell Boulevard on-ramp, (iii) increased R300 on-ramp capacity with lane balancing and (iv) a combined effect of R300 on-ramp capacity increase and ramp metering on Brackenfell Boulevard on-ramp. These were modelled to get an indication of flow characteristics and to assess the changes they produce in comparison to the base case.

The analysis of the results shows that intuitive arguments that were made with reference to the effect of the remedial actions hold true. All the remedial actions resulted with varying improvements in the capacity of the network. Increasing the R300 p capacity had

the most impact and reduced the length of delays experienced within the network. The remedial action with the least improvement was implementing Brackenfell Boulevard on-ramp meter. The results were supported by the output of the regression analysis which suggested higher improved flows when the R300 on-ramp capacity is improved.

Although the core objective of the research was to define and understand the traffic flow behaviour around unconventional weaving, by analysing available video footage and accident statistics, the research also delved into matters of capacity and safety as they are causally linked to weaving behaviour.

With a higher capacity on the freeway there is restricted movement and no free flow of vehicles. The availability of gaps for changing lanes is also reduced with increased flow. For this reason, late acceptance of available gaps occurs leading to increased accident rates and also unconventional weaving. For example, on one of the observed sections, vehicles entering the freeway via the on-ramp waited until late to enter the freeway while vehicles off-ramping also waited until late to exit to the Okavango Boulevard hence resulting in unconventional weaving. The proposed remedial actions yielded improvements inn weaving behaviours. This was evident when the R300 capacity was introduced with lane balancing through incorporating an auxiliary lane that connected the R300 on-ramp to the Okavango Boulevard. In this case vehicles that would have otherwise weaved through traffic from the right lane of the N1 to the exit ramp at a late stage made the move earlier on and kept on to the auxiliary lane hence reducing unconventional weaving. This suggests that weaving within the case study area was not purely due to human behaviour but was also affected by changes on the operation of the road and its geometry.

The limitation of this research is that it failed to accommodate all types of unconventional weaving manoeuvres due to the non-availability of data and because not all manoeuvres could be modelled. Other existing manoeuvres for which data was not available or for which modelling was not completed relate to the following:

- Vehicles on the High Occupancy Vehicles (HOV) lane, which is located on the outer lane, far right in South Africa, are usually forced to make weaving manoeuvres when planning on exiting or entering the freeway. Vehicles tend to manoeuvre from the right outer lane on the freeway to the left hand side located off-ramp or enter the freeway from the left on-ramp to the right hand side outer HOV lane, within a short distance causing weaving directly upstream of the on-ramp and downstream of the off-ramp. An example of this occurrence can be seen on the N2 between Vanguard Drive and Raapensberg Road.

- There is the avoidance or the act of ignoring the solid white line between the freeway and ramps. In some instances, you would find that vehicles would enter the freeway upstream at a solid line while some would try to exit upstream at a solid line. An example of this occurrence is seen on the R300 between van Riebeek Road and Old Paarl road in the Western Cape province of South Africa.
- Weaving could also be a result of avoiding obstacles on the freeway
- In some instances, vehicles will weave through traffic and across lanes to avoid slow moving vehicles, an accident or roadworks.
- Unconventional weaving can also occur due to the driver's familiarity with the section of road. Drivers who tend to frequent the section are more likely to weave in traffic. (Prasetijo *et al*., 2017)

Further research and studies into the causations of weaving with regard to human behaviour and decision making would assist in understanding the causes and effect of unconventional weaving and could lead to increased safety and level of service on the road.

10 REFERENCES

1. Ahmed, K., 1999. Modelling Drivers' Acceleration and Lane Changing Behaviour, USA: Massachusetts Institute of Technology.
2. Balal, E., Cheu, L. R., Gyan-Sarkodie, T. & Miramontes, J., 2014. Analysis of Discretionary Lane Changing Parameters on Freeways. International Journal of Transportation Science and Technology, 3(3), pp. 277-296.
3. Bloomberg, L. & Dale, J., 2000. A Comparison of the VISSIM and CORSIM Traffic Simulation Models on a Congested Network, s.l.: Transport Research Record.
4. Chandler, R. E., Herman, R. & Montroll, E. W., 1958. Traffic Dynamics: Studies in car-following. Operations Research, 6(2), pp. 165-184.
5. Danquah, S. B., 2010. *Spatial and temporal analysis of traffic flows in the City of Almelo: in search for macroscopic fundamental diagram (MDF),* Master's Thesis, Netherlands: University of Twente.
6. Edie, L. C., 1961. Car-Following and steady state theory for noncongested traffic. Operations Research, 9(1), pp. 66-76.
7. Elefteriadou, L., 2014. Modelling Vehicle interactions and the Movement of Groups of Vehicles. In: S. O. a. i. Application, ed. An Introduction to Traffic Flow Theory. New York: Springer Science +Business Media, pp. 31-58.
8. Gao, Y., 2008. *Calibration and comparison of the VISSIM and*. INTEGRATION microscopic traffic simulation models. Master's Thesis. Virginia: Virginia Polytechnic Institute and State University.
9. Gazis, D. C., Herman, R. & Potts, R. B., 1959. Car Following Theory of Steady State Traffic Flow. Operations Research, 9(1), pp. 499-505.
10. Gazis, D. C., Herman, R. & Rotherly , R. W., 1961. Nonlinear follow the leader model for traffic flow. Operations Research, 9(4), pp. 545-567.
11. Gipps, P. G., 1986. A Model for the Structure of Lane-changing decisions. Transportation Research Part B, 20(5), pp. 403-414.

12. Golob, T. F., Recker, W. W. & Alvarez, V. M., 2003. Safety aspects of freeway weaving sections. *Transport Research Part A,* Volume 38, pp. 35-51.
13. Halati, A., Lieu, H. & Walker, S., 1997. CORSIM - CORRIDOR TRAFFIC SIMULATION MODEL, Illinois: Transport Research Board.
14. Halati, A., Lieu, H. & Walker, S., 1997. CORSIM-Corridor Traffic Simulation Model, Washington DC: 76th Transportation Research Board Meeting.
15. HCM: *Highway Capacity Manual*. (1950). Washington: Highway Research Board.
16. HCM: *Highway Capacity Manual*. (1965). Washington: Transportation Research Board.
17. HCM: *Highway Capacity Manual*. (1985). Washington: Transportation Research Board.
18. HCM: *Highway Capacity Manual*. (2000). Washington: Transportation Research Board.
19. HCM: *Highway Capacity Manual*. (2010). Washington: Transportation Research Board.
20. Herman, R. & Rothery, R.W., 1963. Car following and steady state flow, *Proceedings of the Second International Symposium on the Theory of Road and Traffic Flow,* London.
21. Hidas, P., 2005. Lane changing and merging under congested. WIT Transactions on The Built Environment, Volume 77, pp. 779-788.
22. Higgs, B. J., 2011. *Application of naturalistic truck driving data to analyse and improve car following.* PhD Dissertation. Virginia: Virginia Polytechnic Institute and State University.
23. Jack E. Leisch & Associates, 1984. *Procedure for analysis and design of weaving sections,* Illinois: Federal highway administration.
24. Kita, H., 1999. A Merging- Giveaway Interaction Model of Cars in Merging Section: A Game Theoretic Analysis. *Transportation Research,* Volume 33, pp. 305-312.
25. Kou, C.-C. & Machemehl, R. B., 1997. *Modelling Driver Behavious During Metge Maneuvres,* Austin: University of Texas.
26. Kusuma, A., 2015. *Modelling Driving Behaviour at Motorway Weaving Sections,* Leeds: University of Leeds.
27. Kwon, E., Lau, R. & Aswegan, J., 2000. Maximum Possible Weaving Traffic Volume for Effective Operations of Ramp Weave Areas. *Transportation Research Record,* Volume 1727, pp. 132-141.

28. Liu, H. X., Xin, W., Adam, Z. & Ban, J., 2007. A Game Theoretical Approach for Modelling Merging and Yielding Behaviour at Freeways on-ramp Sections. In: Transportation and Traffic Theory. London: Elservier, pp. 197-211.

29. Meng, L., 2006. *Modelling the effects of road traffic safety measures.,* Netherlands: Acident Analysis and Prevention.

30. Mu, R., 2013. *Prediction and Analysis on Micro-Cars',* s.l.: Nagoyi University.

31. Ostrom, B., Leiman, L. & May, A. D., 1993. Suggested Procedures for Analyzing Freeway Weaving Sections. *Transportation Research Record: Journal of the Transportation Research Board,* pp. 42-48.

32. Park B. & Won, J., 2006. Microscopic Simulation Model Calibration and Validation Handbook, Virginia Richmond: VTRC.

33. Prasetijo, J., Baba, I., Nurul E.A.A. and Alvin, J.L.M.S., 2018. *Weaving length and lane-changing behavior at two-sided weaving section along federal road FT050: jalan kluang-ayer hitam.* MATEC Web of Conferences, Vol. 181: EDP Sciences.

34. PTV AG, 2011. VISSIM 5.30-05 User Manual, Karlsruhe, Germany: PTV-AG.

35. Rakha , H. & Crowther, B., 2002. Comparison of Greenshields, Pipes, and Van Aerde Car Changing Behaviour in Weaving Sections. Transportation Research Board, Volume 1802, pp. 248-262.

36. Rakha, H. & Crowther, B., 2002. A Comparison of the Greenshields, Pipes, and Van Aerde Car-Following and Traffic Stream Models, s.l.: Transportation Research Record Journal of the Transportation Research Board.

37. Rakha, H. & Crowther, B., 2003. Comparison and Calibration of FRESIM and INTEGRATION Steady State Car-Following Behaviour. Transportation Research, 37(A), pp. 1-27.

38. Rakha, H. & Zhang, Y., 2004. Integration 2.30 Framework for Modelling Lane Changing Behavior in Weaving Sections. *Transportation Research Record: Journal of the Transportation Research Board,* pp. 140-149.

39. Reilly, W., Kell, J. H. & Johnson, P. J., 1984. *Weaving Analysis Procedures for the New Highway Capacity Manual,* JHK and associates.

40. Richard, W. G., John, C. M. & David, K. O., 2001. *Weave Analysis and Performance: The Washington State Case Study,* Washington: Washington State Department of Transportation.
41. Sarvi, M., Ejtemai, O. & Zavabeti, A., 2011. Modelling freeway weaving manoeuvre. Adelaide, Australasian Transport Reserach Forum.
42. Skabardonis, A. & Kim, A., 2010. *Weaving Analysis, Evaluation and Refinement,* PATH Research Report UCB-ITS-PRR-2010-19, California: University of California, Berkeley.
43. Skabardonis, A., Cassidy, M., May, A. D. & Cohen, S., 1989. Application of Simulation to Evaluate the Operation of Major Freeway Weaving Sections. *Transportation Research Record,* Volume 1225, pp. 91-98.
44. Soria, I. S., 2010. *Assessment of Car Following Models Using Field Data,* Florida: University of Florida.
45. Subramanian, H., 1994. Estimation of Car-Following Models, Massachusetts: MIT.
46. Toledo, T., Choudhury, C. & Ben-Akiva, M., 2005. Lane Changing Model with Explicit Target Lane Choice. Transportation Research Record, Volume 1934, pp. 157-165.
47. Treiber, M. & Kesting A, 2013. In: Berlin Heldeberg: Springer-Verlag .
48. van-Wageningen-Kessels, F., van Lint, H., Vuik, K. & Hoogendoorn, S., 2015. Genealogy of traffic flow models. Euro J Transp Logist, Volume 4, pp. 445-473.
49. Wang, X., Luo, Y., Qiu, T. Z. & Yan, X., 2014. Capacity estimation for weaving segments using a lane changing model. *Transportation Research Record: Journal of the Transportation Research Board,* pp. 94-102.
50. Wei , H., Lee, J., Li, Q. & Li, C., 2000. Observation based lane-vehicle assignment hierarchy. Microscopic simulation on urban street network. *Journal of the Transportation Research Board,* Volume 1710, pp. 96-103.
51. Wei, N. I. & Wanjing, M. A., 2013. Simulation-Based Study on a Lane Assignment Approach for. Social and Behavioral Sciences, Volume 96, pp. 528-537.
52. Yang, Q. & Koutsopoulos, H. N., 1996. A Microscopic Traffic Simulator for Evaluation of Dynamic Traffic Management Systems. Transport Research Part C: Emerging Technologies, 4(3), pp. 113-129.

53. Zhang, Y., 2005. Capacity modelling of freeway weaving sections, PhD Dissertation. Virginia: Virginia Polytechnic Institute and State University.

54. Zhaoyang , L. U. & Qiang, M., 2013. Analysis of traffic speed-density regression models. Singapore, Proceedings of the *Eastern Asia Society for Transportation Studies*, Vol.9, 2013

ANNEXURE A: RESULTS OF THE REGRESSION ANALYSIS

GREENSHIELDS

Table 10-1: Greenshields Model Regression Analysis Output

Regression Statistics	
Multiple R	0,966586
R Square	0,934288
Adjusted R Square	0,933731
Standard Error	10,55596
Observations	120

	Coefficients	*Standard Error*	*t Stat*	*Lower 95%*	*Upper 95%*	*Lower 95,0%*	*Upper 95,0%*
Intercept	119,4556	1,311485	91,08425	116,8585	122,0527	116,8585	122,0527
X Variable 1	-1,65396	0,04038	-40,9598	-1,73392	-1,574	-1,73392	-1,574

GREENBERG

Table 10-2: Greenberg Model Regression Analysis Output

Regression Statistics	
Multiple R	0,872528
R Square	0,761306
Adjusted R Square	0,759283
Standard Error	0,80961
Observations	120

	Coefficients	*Standard Error*	*t Stat*	*Lower 95%*	*Upper 95%*	*Lower 95,0%*	*Upper 95,0%*
Intercept	5,062734	0,167447	30,2348	4,731143	5,394325	4,731143	5,394325
X Variable 1	-0,03511	0,00181	-19,3999	-0,0387	-0,03153	-0,0387	-0,03153

UNDERWOOD

Table 10-3: Underwood Model Regression Analysis Output

Regression Statistics	
Multiple R	0,991364
R Square	0,982803
Adjusted R Square	0,982657
Standard Error	3,155885
Observations	120

	Coefficients	*Standard Error*	*t Stat*	*Lower 95%*	*Upper 95%*	*Lower 95,0%*	*Upper 95,0%*
Intercept	165,8047	1,774343	93,44568	162,291	169,3184	162,291	169,3184
X Variable 1	-34,016	0,414229	-82,1188	-34,8363	-33,1957	-34,8363	-33,1957

BELL-SHAPED

Table 10-4: Bell-Shaped Model Regression Analysis Output

Regression Statistics	
Multiple R	0,953922
R Square	0,909968
Adjusted R Square	0,909205
Standard Error	488,4604
Observations	120

	Coefficients	*Standard Error*	*t Stat*	*P-value*	*Lower 95%*	*Upper 95%*	*Lower 95,0%*	*Upper 95,0%*
Intercept	10413,2	274,6286	37,91739	6,29E-68	9869,362	10957,04	9869,362	10957,04
X Variable 1	-2214,13	64,11338	-34,5346	1,57E-63	-2341,09	-2087,17	-2341,09	-2087,17

ANNEXURE B: FUNDAMENTAL DIAGRAM OF TRAFFIC FLOW FOR ALL LOCATIONS AND REMEDIAL ACTIONS

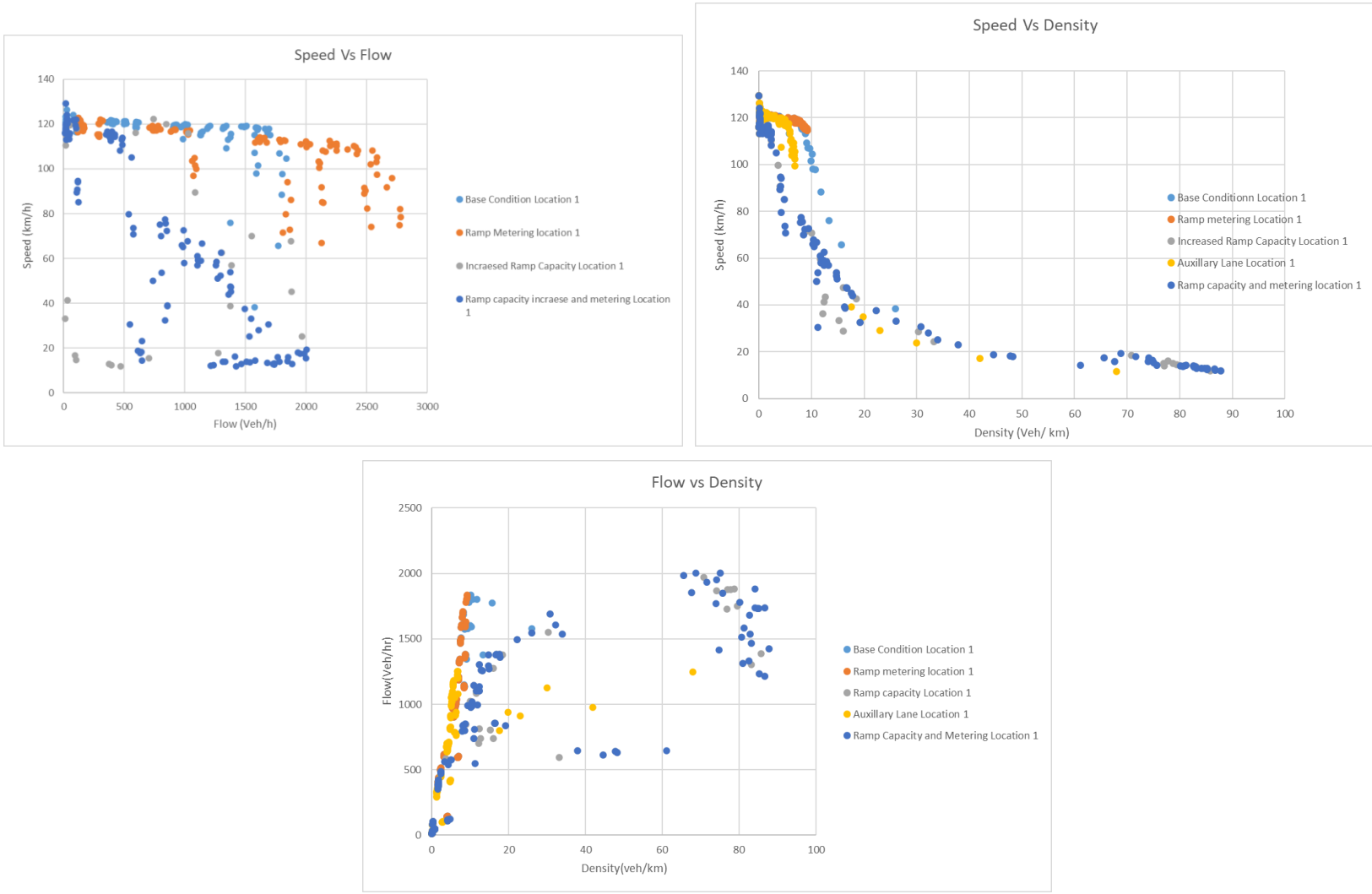

Fundamental flow diagram for Location 1

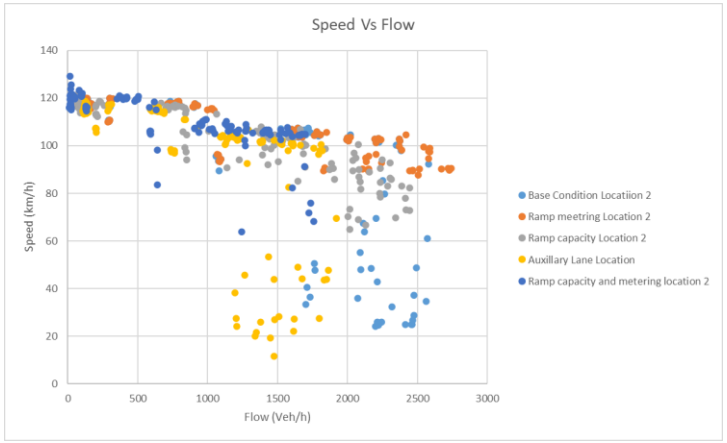

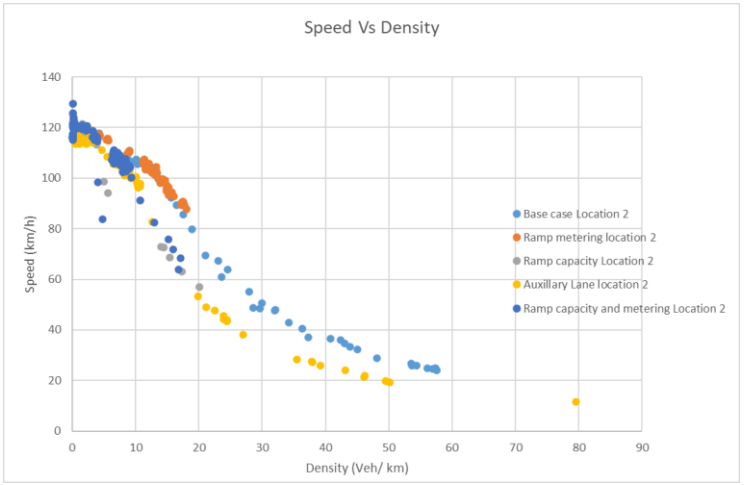

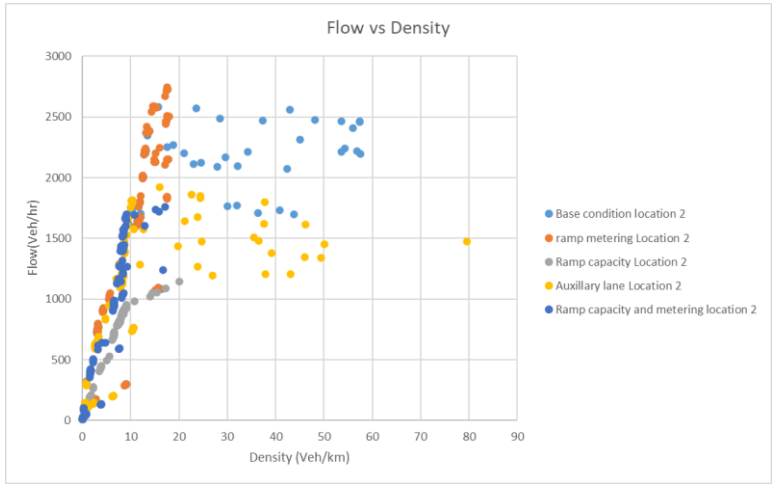

Fundamental flow diagram for Location 2

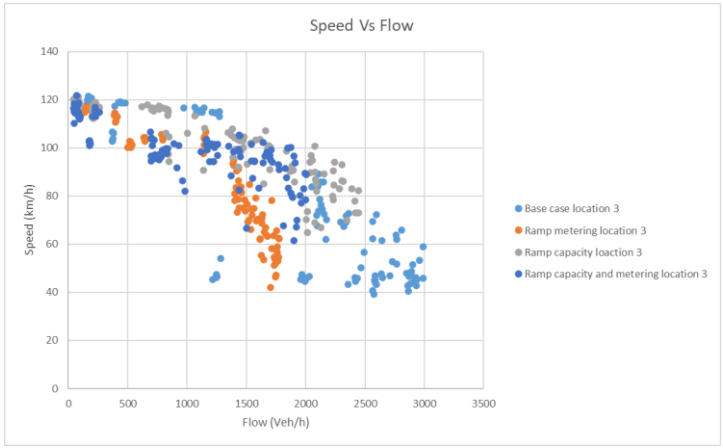

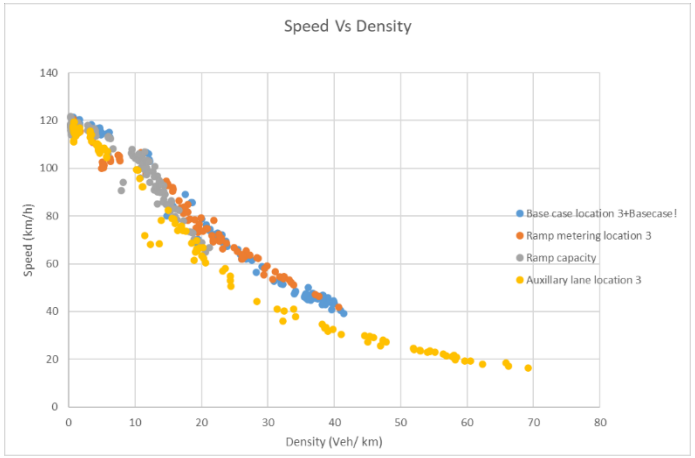

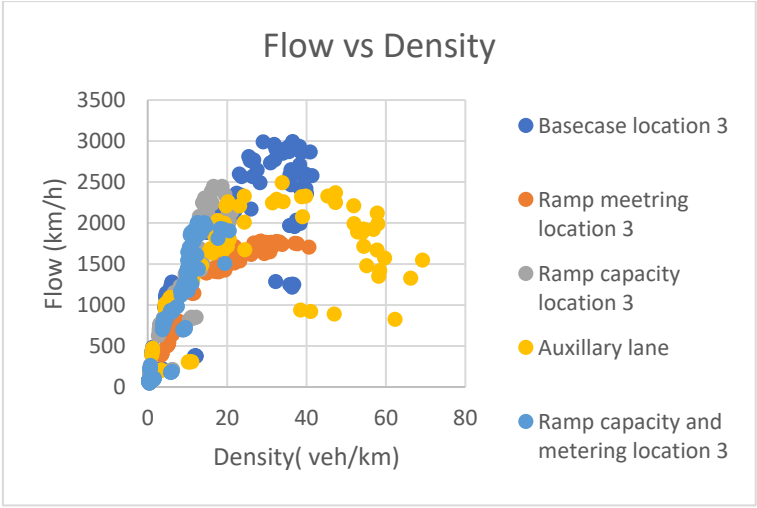

Fundamental flow diagram for Location 3

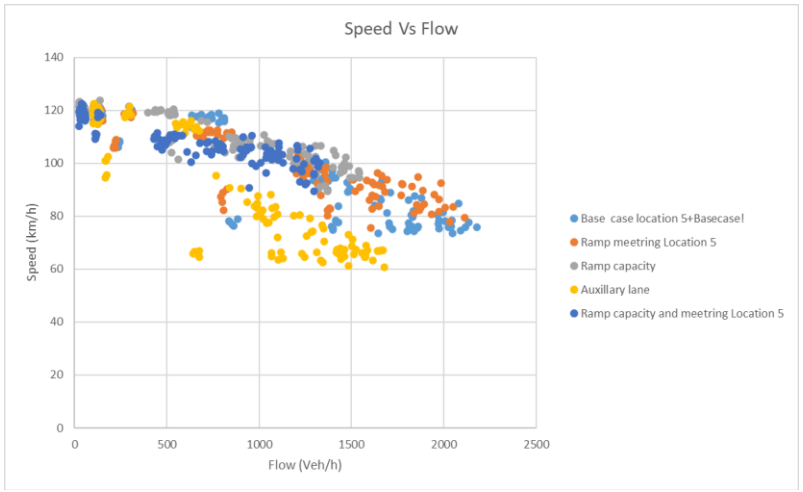

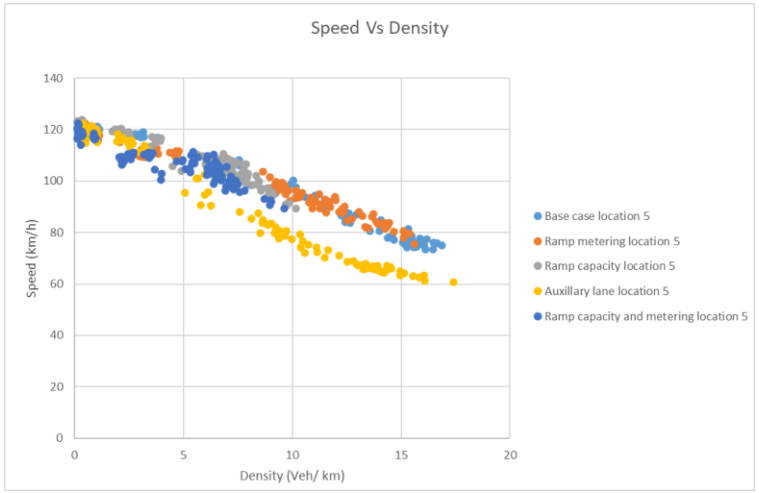

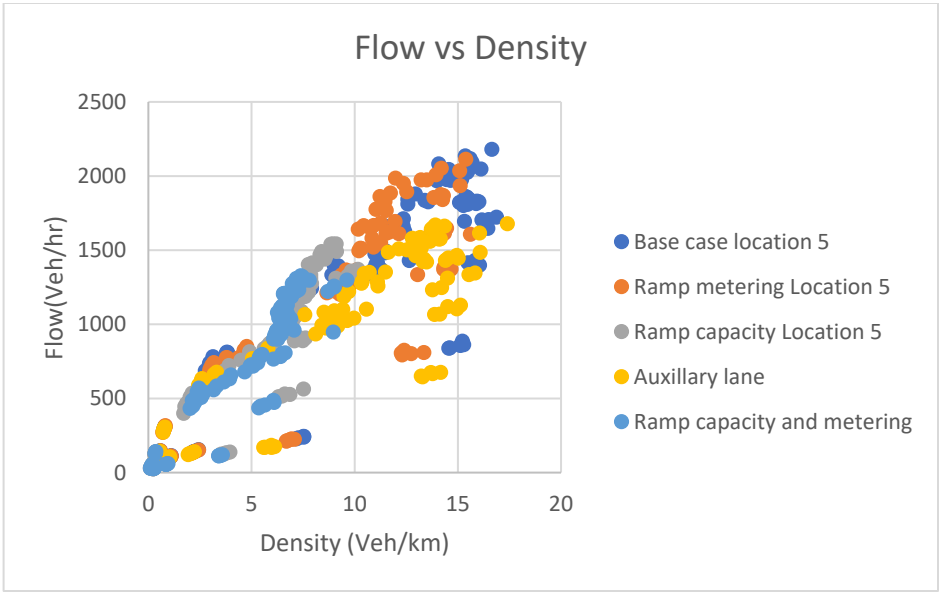

Fundamental flow diagram for Location 5

ANNEXURE C: FUNDAMENTAL DIAGRAM OF TRAFFIC FLOW FOR EACH REMEDIAL ACTION

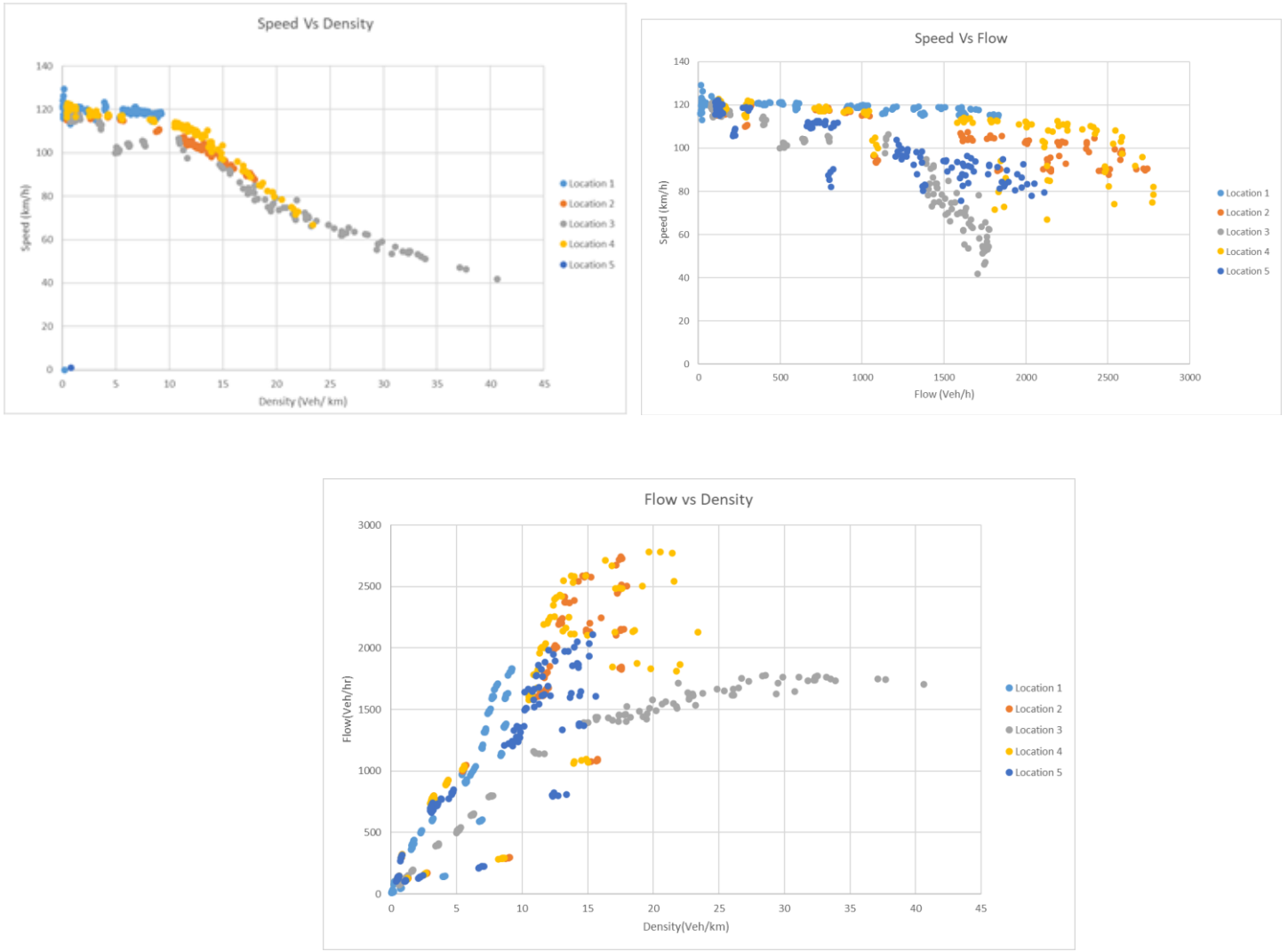

Figure 10-1: The effect of ramp metering

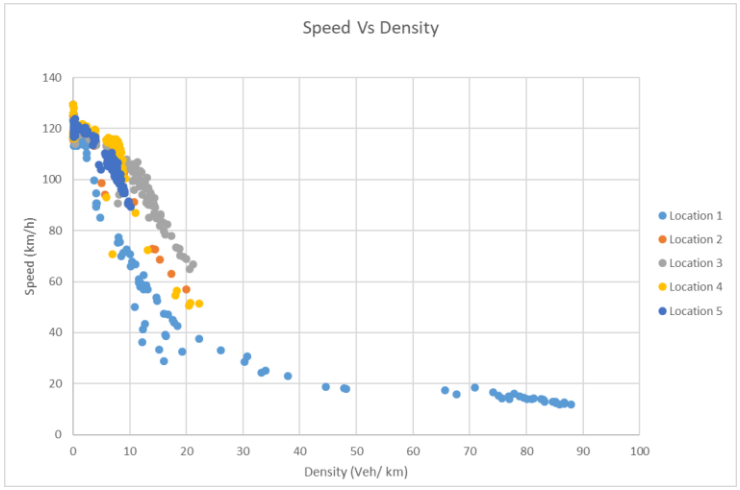

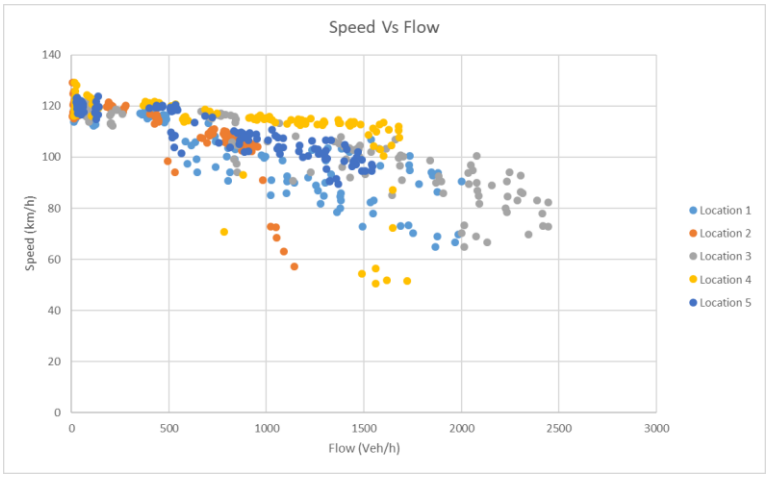

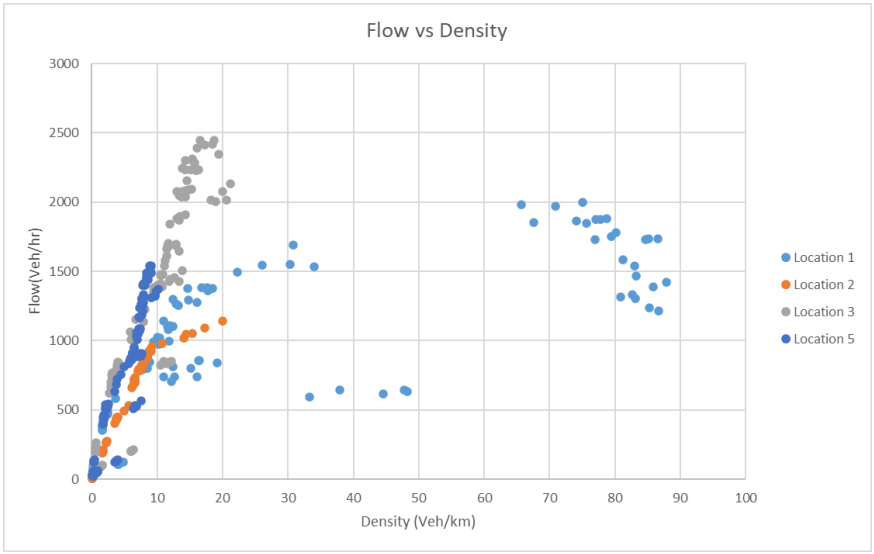

Figure 10-2: Effect of R300 capacity increase on to the traffic flow

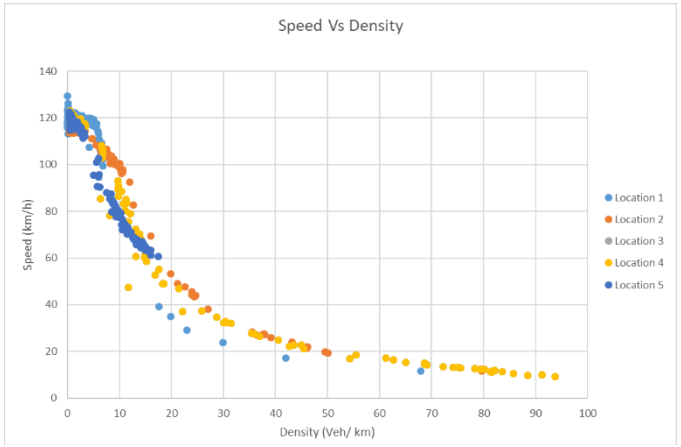

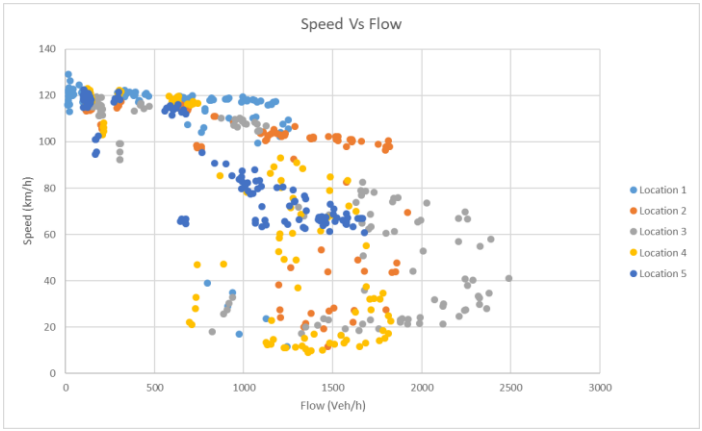

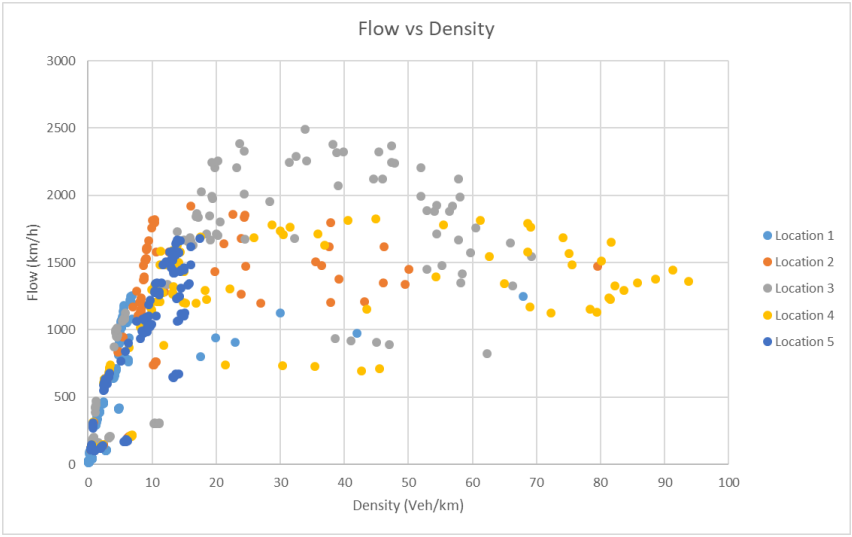

Figure 10-3: Effect of adding an axillary lane to the traffic flow

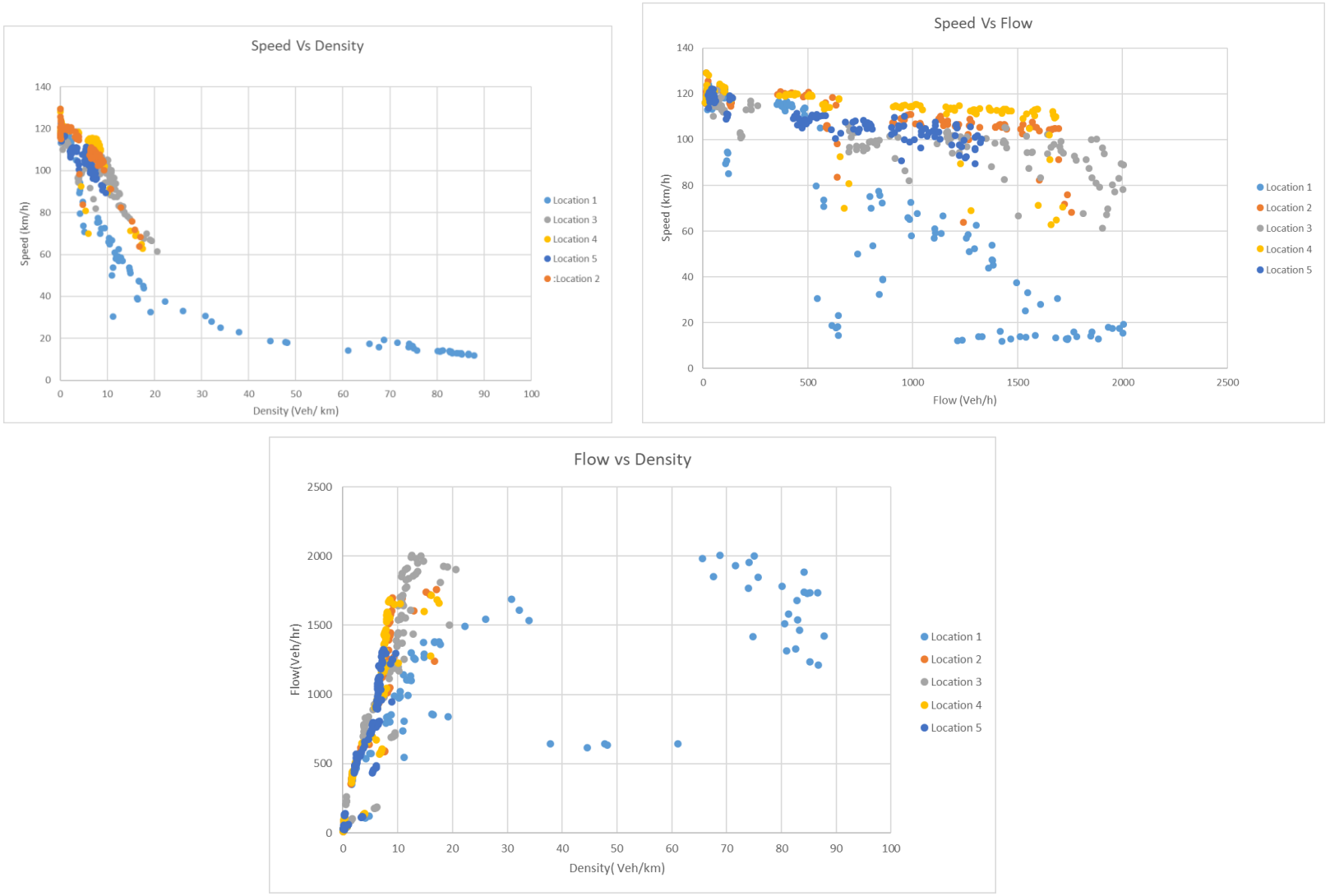

Figure 10-4: Combined effect of ramp metering and R300 capacity increase